ASSESSMENT OF STORMWATER INFRASTRUCTURE FOR MITIGATING FLOODING AND NON-POINT SOURCE POLLUTION

By

HELIA FARZANEH

A Thesis

Submitted to the Faculty of University of Texas at Arlington

In Partial Fulfillment of the Requirements for the degree of

Master of Science

Department of Civil Engineering

Arlington, Texas

December 2021

Supervising Committee:

Dr. Yu Zhang, supervising professor

Dr. Habib Ahmari

Dr. Jessica Eisma

To my beloved husband

Hadi

to my parents

Fereshteh and Kourosh

And to my sisters

Ava and Hanna

ACKNOWLEDGMENTS

First, I would like to offer my sincere gratitude to my mentor and advisor, Yu Zhang. Over the last couple of years, I have been benefited from his knowledge and wisdom immensely. Professor Zhang provided me with invaluable guidance while educating me to be an independent researcher. One simply cannot wish for a better advisor.

I would like to appreciate my examination committee members, Professor Habib Ahmari and Professor Jessica Eisma, for their constant support and invaluable guidance and comments during my M.Sc. studies, making this thesis more philosophical.

I would like to thank Professor Qin Qian from Lamar University and Dr. Michael Schramm from Texas Water Resources Institute for their friendship and advice. I have been very fortunate to have the opportunity to collaborate with them. The friends that I made during this time made this journey very enjoyable. I would like to thank Nabin Basnet, Vaqef Ghazvinian, Babak Alizadeh, Jose Velasquez, Angie Fealy, and Qazi Ashique Mowla.

This thesis has not been completed without the support of my parents. The emotional support of my father for two years has always been the source of enthusiasm. There are not enough words to express how thankful I am. My mother, whom I thank for her unconditional love and devotion during all these years. She has introduced me to the definition of “motivation” with all the sacrifices she has made to help me reach my professional achievements. I would also like to thank my older and twin sisters for being role models in my personal life.

Lastly, I offer my deepest gratitude to my beloved husband, Hadi. He has always been caring and loving during the last two years. I cannot express how thankful I am for all these years, being compassionate, and helping deal with crucial times.

TABLE OF CONTENTS

LIST OF TABLES

LIST OF FIGURES

ABSTRACT

Flooding is the top natural hazard impacting coastal and inland communities in Texas. Beyond its destructive impact on rising waters in communities, flooding-induced stormwater negatively affects the quality of large bodies of water. Stormwater runs over land, washes off pollutants, and deposits them into rivers which causes water quality issues in bays and estuaries. In addition, the stormwater increases nutrients, sediments, oxygen-demanding substances, pathogens, and toxins which results in hypoxia in the aquatic system. During the last 5-6 years, severe storm events such as Tropical Storm Beta (September 2020), Tropical Storm Imelda (September 2019), Hurricane Harvey (August 2017) have caused a fatality and billions in damages along the Gulf Coast region. These events have shown that stormwater and wastewater infrastructures for many coastal and near-coastal communities are inadequately prepared for the frequency and magnitude of these storms. Infrastructure upgrades are costly to implement and maintain. Many smaller urban and rural coastal communities are unlikely to have the resources to complete infrastructure upgrades that will enhance their resiliency during flooding events.

Texas has been working to implement the Coastal Nonpoint Source (CNPS) Program, which includes promoting and facilitating the implementation of stormwater best management practices (known as BMPs) in small urban and urbanizing coastal areas. These practices are distinguished by whether engineering (structural) or administrative (nonstructural) procedures are taken. In this study, BMPs as techniques, practices, or structural controls are used to manage and mitigate the quantity and quality of stormwater runoff to the greatest extent possible. To do this, between different types of BMPs such as wet detention ponds, dry detention pond, swales, constructed wetlands, and levees, the most effective BMPs have been selected. For application of these BMPs, three scenarios are defined. This work develops a decision framework to provide

opportunities for coastal communities to assess the performance of stormwater infrastructures vulnerable to flooding risk using up-to-date precipitation frequency estimates and determine the most cost-effective scenario to alleviate stormwater runoff and downstream water quality issues arising from flood events. The resultant scenario is used to appraise the cost-effectiveness of stormwater BMPs in mitigating the impacts of flooding on water quality in the flood-prone lower Neches River region. The analysis yields a table of the cost of BMP implementation, estimate flood risk reductions in terms of stormwater peak flow reduction, and potential improvements to water quality measures.

1. INTRODUCTION

1.1 Background

Climate change is anticipated to aggravate the hydrological cycle, thereby increasing the danger of floods and droughts in the next decades (Huntington et al., 2006; Lavers et al., 2015; Trenberth, 2011). Across the United States, local communities are increasingly taking on the burden of dealing with these recurrent floods. Flooding has consistently ranked as the most dangerous natural hazard for coastal and inland areas in the Southeastern region of Texas. In addition, recent research has revealed that slow-moving tropical cyclones are becoming more common in the United States. Increased ocean heat content increases the precipitation potential of severe storms and catastrophic flooding along the Gulf Coast (Kossin, 2018).

Water has flooded Houston, TX on numerous occasions in the distant and recent past, most recently on Memorial Day 2015, Tax Day 2016, Harvey 2017, and Imelda 2019. The latter storm event has been marked as one of the top five wettest tropical cyclones ever to hit the region, resulting in a maximum precipitation total of 43.39 inches on the region. In addition, hurricane Harvey poured an almost inconceivable 60.58 inches of rain near the city of Nederland, TX in Jefferson County for 5 to 6 days (Blake & Zelinsky, 2018), which is more than the county's typical precipitation of 60 inches per year (Https://Www.Weather.Gov/Media/Hgx/Climate/Summary/August_Climate_Article_2012.Pdf, n.d.). As a result of these and other severe rain events in Southeast Texas over the previous five years, significant disruption and damage have been done.

Starting in the town of Colfax in east-central Texas, the Neches River flows southward until it pours into Sabine Lake in southeast-central Texas. In total, the river flows for around 416 miles and drains at an area of approximately 10,011 square miles, according to the Texas Parks and

Wildlife Department. The watershed of the Neches River generates approximately 6,000,000 acre-feet of runoff per year. The river runs through several counties and is regarded as a valuable source of water and recreational opportunities by local communities. The Neches River is also a vital component of the regional economy of Southeast Texas, and it serves as a transportation corridor. According to its mission statement, the Port of Beaumont also serves to help both the local economy and the worldwide trade sector. An economic impact analysis conducted by the Texas Comptroller's office in 2018 found that Beaumont's port contributed $12.6 billion to the state's gross domestic product and $18.8 billion in direct foreign trade value (Hegar, 2018).

Flooding has always been a problem in this area along the Neches River's eastern bank. With the climate growing increasingly unstable and the frequency and power of tropical cyclones increasing over time, disasters like Hurricane Harvey are almost certain to become more frequent and severe. In order to prevent flood damage to residential dwellings and industrial assets along the Neches River, it is in the best interests of the inhabitants and businesses to implement flood mitigation measures. Structural approaches have overshadowed the history of flood mitigation in the United States since the Mississippi River disaster of 1927 (Birkland et al., 2003). Communities are taking crucial efforts to limit the amount of property damage and human casualties caused by localized flooding by adopting and implementing structural or nonstructural mitigation methods. These approaches are distinguished by whether engineering or administrative procedures are used (Dalton et al., 1996). Building seawalls, levees, channels, and revetments are some of the most common structural measures used to regulate flooding or protect human populations from flooding. Nonstructural approaches, on the other hand, are based on the adaptation of human activities and communities to mitigate flood damage, with measures such as directing land use away from flood-prone areas, communicating mitigation information, protecting sensitive areas, and developing insurance schemes to distribute the risk information (Few, 2003). It is common practice to use a combination of structural and nonstructural mitigation methods as part of a single jurisdictional flood program.

As BMPs become more vital to urban stormwater management, the need for tools to assist designers in selecting the most desirable BMPs that generate the most cost-effective stormwater solutions grows. Many water resource management issues can benefit from using strategic plans to find and evaluate the most cost-effective solutions. For example, the Stormwater Management Model (SWMM) and cost-effective solutions can produce viable strategies for deploying BMPs, specifically detention ponds, to treat stormwater in urban watersheds (Damodaram & Zechman, 2013; Giacomoni & Joseph, 2017).

1.2 Research Objectives

Best management practice methods can be integrated into cost-effective stormwater management plans using this study's realistic scenario-based decision-support tool. The objectives for this study are:

- To upgrade the stormwater infrastructures through defining three scenarios for the location of the BMPs and to perform the cost-benefit analysis of these three scenarios.
- Integrate a micro-organism prediction in urban stormwater (MOPUS) model with SWMM model to simulate bacteria loads in stormwater catchments.

1.3 Organization of Thesis

The rest of the thesis is organized as:

Chapter 2: Literature Review summarizes research and developments in urban stormwater issues, the use of BMP infrastructure implementation regarding water quantity and water quality improvements, and strategies that have been developed for highlighting the cost-effectiveness attributes of BMPs.

Chapter 3: Methodology outlines the processes used to create a decision-support tool for stormwater best management practices. This chapter describes the procedures used to develop a framework model to carry out the water quantity and quality attributes.

Chapter 4: Case Study highlights a case study using the developed tool.

Chapter 5: Results describes and discusses the structure and function of the user interface for the developed decision-support tool. This chapter also compiles, presents, and discusses the relevant results of the case study and sensitivity analysis.

Chapter 6: Conclusions contains a summary of the conclusions drawn from this study and a discussion of how the research objectives were satisfied. Also in Chapter 5 are recommendations for future research. Following Chapter 5 are references to works cited and appendices that provide supplementary data and methodological details.

2. LITERATURE REVIEW

2.1 Best Management Practices

When managing urban stormwater runoff, Best Management Practices (BMPs) as structural mitigation strategies have traditionally been used to achieve the greatest amount of success. BMPs are techniques, practices, or structural controls used to manage and mitigate the quantity and quality of stormwater runoff to the greatest extent possible (Swama Muthukrishnan et al., 2006). In addition, studies that compare watersheds with and without BMPs help further support the usage of BMPs (Bedan & Clausen, 2009).

Dry detention ponds, wet retention ponds, swales, and infiltration systems are examples of structural BMPs that may be used to regulate water amount (Swarna Muthukrishnan & Selvakumar, 2006). Detention and retention ponds are composed of a basin with an outlet structure that limits the quantity of water that can flow through it to a controlled level. When stormwater runoff events occur, limiting the outflow causes stormwater to be trapped and stored. Detention ponds are devoid of water between storm events, while retention ponds contain a constant pool of water throughout the year. In a retention pond, when runoff arrives, a considerable percentage of the retained water that the permanent pool had confined is displaced and leaves via the primary outflow. When a new precipitation event happens, the water is maintained until the next one occurs. The retention pond may temporarily hold runoff over the permanent pool level, up to and including the emergency spillway, during times of significant precipitation occurrences

Historically, BMPs (mainly wet and dry ponds) have been used centrally and near to stream channels positioned away from development to reduce peak discharge and minimize hydrologic modifications relative to pre-urbanized circumstances; yet, hydrologic difficulties have persisted. Recently, BMPs have started to be applied in a decentralized way to regulate stormwater runoff on the catchment and closer to its source, with a concentration on infiltration, catchment retention, and interaction with urban planning (Davis, 2005; Roy et al., 2008). However, despite the early adoption of distributed BMPs, broad usage has been hampered in part by a scarcity of catchment-scale performance data (Davis, 2005; Hamel et al., 2013; Roy et al., 2008).

2.1.1 Water Quantity

With a primary emphasis on water quantity management, the typical urban drainage system neglects other essential considerations, such as runoff quality, recreational value, and ecological preservation. Therefore, researchers in industrialized nations have investigated a variety of systematic urban stormwater control strategies, including BMPs (Environmental Protection Agency, 2004), sustainable urban drainage systems (Napier et al., 2009), and water-sensitive urban design (Coombes et al., 2000). BMPs are the most convenient application of sustainable drainage and are extensively employed in the USA (D'Arcy & Frost, 2001). In addition, there is a wealth of literature on the ecological benefits of BMPs for stormwater management, including the use of green roofs (Berndtsson, 2010; Vijayaraghavan et al., 2012), vegetated filter strips (Abu-Zreig et al., 2004), bioretention (Kim et al., 2012), and porous pavement (Scholz & Grabowiecki, 2007), and constructed wetlands (M Karamouz et al., 2018; Mohammad Karamouz et al., 2020; Mohammad Karamouz & Farzaneh, 2020).

Reduced peak flows may be achieved by either increasing the hydraulic residence time or decreasing the amount of runoff via storage. Flood control has traditionally been the primary emphasis of stormwater management, which has traditionally been accomplished via detention ponds, which are intended to hold and slowly release huge amounts of runoff. On the other hand, detention ponds are not intended to alleviate changes in the long-term flow regime. Detention ponds lower peak flows, but they can drastically alter the timing and form of storm hydrographs because they discharge strong flows over a long period as the stored runoff makes its way to the downstream reach of the pond. In other cases, smaller storms may travel over ponds without being attenuated (Roesner et al., 2001). In order to reduce the peak flow at the watershed outflow, decision support systems have been developed and implemented to build detention ponds (Harrell & Ranjithan, 2003; Zhen et al., 2004).

2.1.2 Water Quality

Increased urban runoff and hydrologic changes resulting from urbanization and climate change also negatively impact water quality. Runoff from urban areas conveys pollution from several pollutants that have been deposited on urban surfaces as a result of direct human activity (such as building and septic systems), as well as air deposition (such as vehicle and coal power plant emissions) (Shaver et al., 2007). Also, many sections of the world suffer from water quality deterioration caused by non-point source pollution (NPS) (Shaw, 2003). Since stormwater runoff is a significant portion of urban NPS, it contains high quantities of biological pollutants associated with disease outbreaks, aquatic biological toxicity, and water quality degradation, among other negative impacts (McIntyre et al., 2015). It is also important to be concerned about pollution by microbes, particularly pathogens, which are believed to be a primary source of deterioration of rivers, streams, and estuaries worldwide (Vitro et al., 2017).

Consequently, researching micro-organisms in urban stormwater is very important for water quality control and stormwater re-use applications. As of right now, it is not feasible to simulate hundreds of different micro-organisms that may be present in stormwater. A great deal of research has been dedicated to the simulation of fecal indicator bacteria (FIB), which is often employed to indicate microbiological deterioration of water. Previous research has been mostly on FIB simulations in rivers, lakes, and rural runoff (Haydon & Deletic, 2006; He & He, 2008). Many studies have indicated that models applied for water catchment quality, such as the Soil and Water Assessment (SWAT) tool, are not suitable for modeling FIBs in urban environments (McCarthy et al., 2011). The focus of this study is to systematically implement two approaches for reducing peak flow and treatment of runoff for non-point source pollutants. It is necessary to note that previous studies have assessed the influence of BMPs incorporation on hazard mitigation; however, little attention has been given to the estimation of reduction in bacteria concentration through the application of BMPs.

2.2 Cost-Effective Analysis

Prior studies have evaluated the cost-effectiveness of BMPs with various stormwater models and methodologies because the cost of implementing BMPs limits their practical application (Gassman et al., 2010; Guto et al., 2011; Panagopoulos et al., 2011; Strauss et al., 2007). Liu et al. (Liu et al., 2013) used life cycle assessment modeling to examine the trade-offs between water quality improvements from BMP implementation and gray alternatives of stormwater infrastructures. They found that bioretention could achieve water quality improvement goals while incurring the least climate and economic costs. According to Chui et al. (Chui et al., 2016), the cost-effectiveness of certain BMP designs in response to significant storm occurrences is evaluated using life cycle costing. While life cycle costing discloses the spending analysis, life cycle assessment may investigate the environmental sustainability, and the two studies work well together as a complement (Vineyard et al., 2015). As a result, this research evaluated the cost-effectiveness of a bioretention system for stormwater management coupling the attributes above rather than hydrologic performance as the primary metrics. The United States Department of

Agriculture has experimented on a watershed located in Pennsylvania that indicated that BMPs decreased pollutant loads by up to 56 percent while increasing net income by as much as 109 percent every year (Srivastava et al., 2002). To this end, this study aims to carry out a scenario-based cost-effective analysis of BMP implementation based on peak flow reduction and bacteria concentration diminution at a watershed scale.

3. METHODOLOGY

3.1 Case Study

The lower 20 miles of the Neches River from the confluence of Pine Island Bayou to the intersection of Interstate Highway 10 was used in this thesis to evaluate the impact of the stormwater runoff and downstream water quality issues arising from flood events. The defined section of the Neches River's drainage area is 79.6 square miles, and its watershed is located within the Jefferson, Orange, and Jasper counties of Texas. The breakdown of the area, population, and population density of each county in the study area are listed in **Error! Reference source not found.**. The Neches River flows to the Sabine Lake and Galveston Bay, one of the most important commercial fisheries and ports in the western Gulf of Mexico. **Error! Reference source not found.** shows the location of the area of interest within the Neches River watershed. In this figure, the outline of the Neches River is sketched in purple line within the study area.

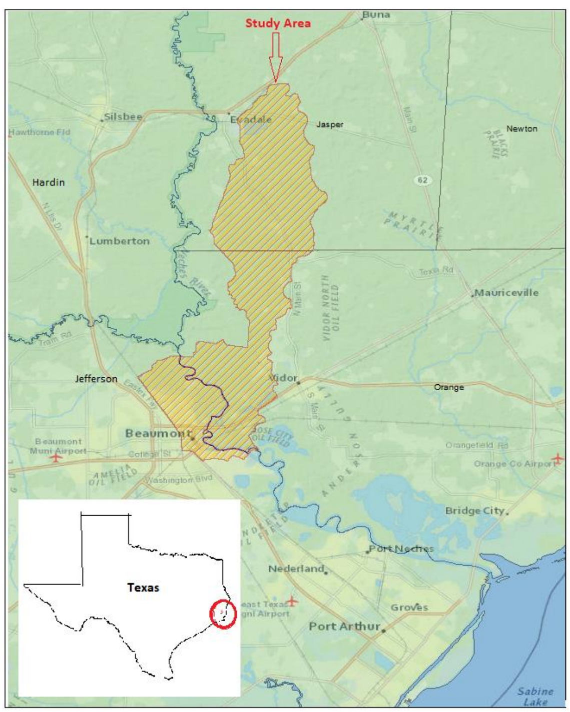

Figure 3-1. Location map of the study area

Table 3-1. Demography of the study area by county

County Name	Area (mi^2)	Total Population (2010)	Population Density (Total Population /area (mi^2))
Jasper County	36	35710	37
Jefferson County	14	252273	268
Orange County	30	81837	239

Micro-organisms have been identified as the main pollutant affecting the quality of coastal waters, rivers, and urban estuaries. The section of the Neches River used in this study is identified as bacteria impaired by the Texas Integrated Report of Surface Water Quality for Clean Water Act Sections 305(b) and 303(d). Seepage from on-site sewage facilities (OSSFs) is an important source of nutrients and pathogens to the surface waters (Gros et al., 2017). In recent 5 to 6 years, the severe storm events in the vulnerable areas have increased the risk of stormwater infrastructure failure, contributing to the increased aquatic contaminants in the water bodies downstream. Based on the distribution density of OSSFs, this study evaluates the influence of these septic facilities on the surface water quality following extreme weather events such as Hurricane Harvey. In addition, it evaluates the different BMPs for their mitigation.

3.2 Catchment Discretization

Finer-scale planning units included NHDPlus catchments within the HUC8 watershed, a scale at which protection or restoration operations are selected in this study. The primary goal is to create a compatible and hydrologically accurate catchment for each smaller catchment segment using the NHDPlus catchment elevation data. In order to give an equal planning unit size, several NHDPlus catchments have been adjusted. This special discretization has been accomplished by separating extremely large catchments into smaller units or merging extremely tiny catchments with the next bigger catchment. Through this method, a total of 11 discretized catchments representing the whole study area (highlighted in blue) are identified, as shown in Figure 3-2.

This study highlights an existing flaw in the calibration and verification processes as there is no flow gauging station downstream of the catchments and within the tributaries of the Neches River region. Therefore, the gauged catchment (i.e., surrogate watershed highlighted in green), Cow Bayou in Mauriceville, Texas, located close to the area of interest, has a drainage area of 88.9 square miles taken into account in this analysis. Regional data can be used to estimate the parameters of hydrological models for catchments that do not have discharge records. Moreover, it is anticipated that catchments with similar characteristics, including slope, are likely to have similar hydrological responses, and as a result, they may be modeled using similar parameters. A consequence is that the hydrological model parameters can be regionalized following the features of individual catchments. Because of this, overland flow on both pervious and impervious sections of the surrogate watershed has been transferred to a model of the Neches River's watershed, resulting in the manning's factor "*n*" for both pervious and impervious sections.

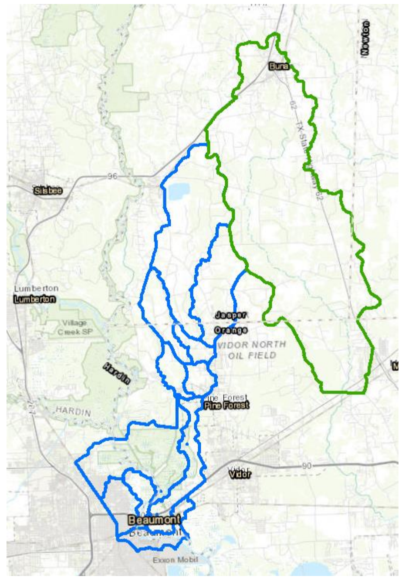

Figure 3-2. The Schematic locations of the area of interest and test catchment.

3.3 On-site Sewage Facilities (OSSFs)

Private residential on-site sewage facilities (OSSFs), commonly referred to as septic systems, consist of various designs based on the physical conditions of the local soil. Typical designs consist of (1) one or more septic tanks and a drainage or distribution field (anaerobic system), and (2) aerobic systems that have an aerated holding tank and often an above-ground sprinkler system for distributing the liquid. In simplest terms, household waste flows into the septic tank or aerated tank, where solids settle out. Then, the liquid portion of the water flows to the distribution system, consisting of buried perforated pipes or an above-ground sprinkler system. Estimates of the number of OSSFs within the General Land Office Texas Coastal Zone portion of the watershed are determined using the TCEQ and Texas A&M AgriLife draft coastal zone OSSF database Figure 3-3. indicates the locations and spatial distributions of OSSFs within each catchment. The detailed information of the number of OSSFs and each catchment area is illustrated in Table 3-2.

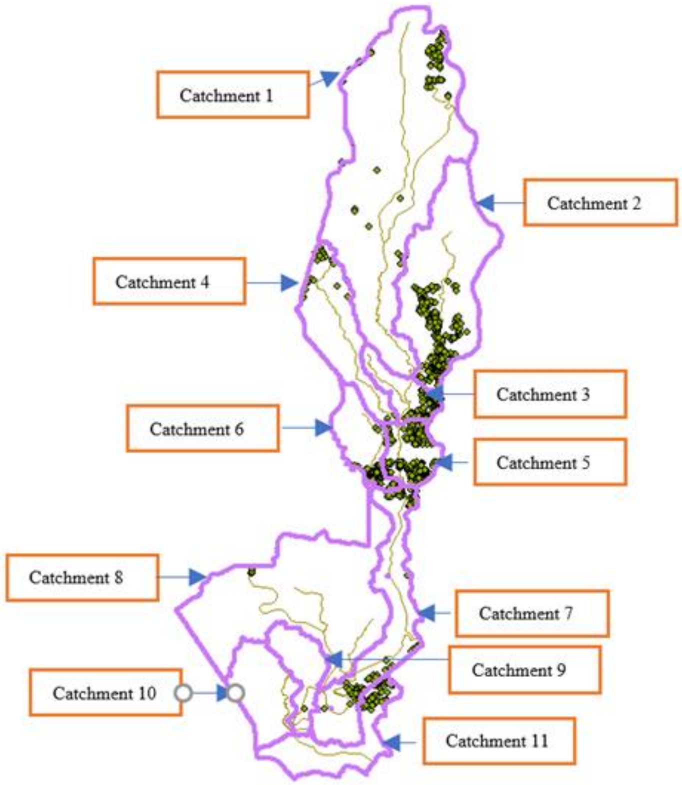

Figure 3-3. Schematics of eleven catchments and designated on-site sewage facilities (OSSFs).

Table 3-2. The area and number of OSSFs in each catchment were obtained from TCEQ and Texas A&M AgriLife drafts coastal zone databases.

Catchments	**Area (mi^2)**	**Number of OSSFs**
Catchment 1	23.31	87
Catchment 2	10.87	289
Catchment 3	5.35	34
Catchment 4	2.08	119
Catchment 5	2.39	125
Catchment 6	2.87	118
Catchment 7	7.15	148
Catchment 8	15.34	9
Catchment 9	2.68	1
Catchment 10	3.91	0
Catchment 11	3.92	118

3.4 Modeling Process Selection

The EPA's Stormwater Management Model (SWMM) was first developed in 1971 and has experienced several major upgrades. The latest version, 5.1.013, released in 2020, consists of a software utility that grants future climate change projections to be combined with modeling. This model is a comprehensive hydrological and water quality simulation model which is developed mainly for urban areas. It could be applied for a single precipitation event or long-term continuous water quantity and water quality simulation. The core simulation phases of the SWMM model are precipitation incorporation and overland and groundwater flow calculation. The overland flow calculation is only considered in this study. Within the SWMM model, the user must decide the mechanisms that regulate infiltration and transport routing. When it comes to calculating infiltration, there are three options: the Horton approach, the Green-Ampt method, and the Curve Number method. As an infiltration method based on curve numbers, the latter method is employed for this study's comparison purposes. The reason is that the curve number method reflects the runoff potential. However, in SWMM, we additionally need to input the percent impervious for each sub-catchment that we are modeling. If we apply the curve number approach to calculate soil infiltration, we are effectively double-counting the impacts of imperviousness on the soil. In addition, the channel flow routing can be accomplished in three ways: steady flow, kinematic wave, and dynamic wave flow routing. To model channel flow routing, the kinematic wave routing method is adopted.

In order to characterize the area of interest in SWMM and calculate infiltration and flow routing characteristics, comprehensive physical data needs to be gathered. Because Geographic Information Systems (GIS) data is widespread and continually improving, much of the physical data required for the SWMM model was readily available as spatial data files at the time of its development. As a result, leveraging GIS datasets for large-scale data collecting proved to be the most efficient way.

Many inputs are necessary to simulate land surfaces, most of which are gathered via the Texas Office of GIS web data portal. ArcGIS was used to view and analyze these data files, which were referred to as layers. The obtained data layers comprise current soil type, land use/land cover, infiltration, and channel flow routing. For further information, a brief introduction to each physical data collection is provided in the following sub-sections.

3.4.1 Soil Type

A variety of soils are categorized in one of seven possible runoff-based potential classes or hydrologic groups. According to the USDA NRCS SSURGO database, these classes are determined by the expected rate of water infiltration when soils are not covered by vegetation, are moist, and receive precipitation from storms that last for an extended period. Three dual classes (A/D, B/D, and C/D) are included in each of the four primary groupings (A, B, C, and D). Soils with dual hydrologic groups suggest that drained regions are allocated the first letter of the hydrologic grouping. Undrained areas are given the second letter of the hydrologic grouping, as shown in the illustration. Thus, only soils are classified as group D in their native state allocated to dual classification systems. Figure 3-4 depicts the spatial distribution of soil hydrologic groups throughout the Neches River basin. Under normal conditions, soil groups C and D are found in the majority of the watershed, indicating that water is infiltrating slowly or very slowly in most of the area. The distribution of different soil group for class of A, C, C/D, and D are 5.4 %, 6.5%, 53.8%, and 34.3%, respectively.

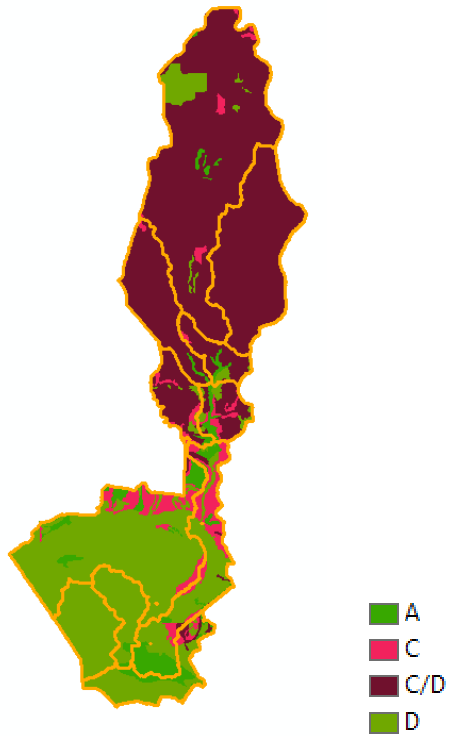

Figure 3-4. Illustration of the soil hydrologic group within the Neches River watershed.

3.4.2 Land Use/Land Cover

The watersheds' land cover was derived from the 2016 National Land Cover Database (NLCD). The Neches River watershed is distinguished by large areas of wetlands and open water. As the watershed extends into Jasper County, the amount of forested land increases in the northern portions of the watershed (Figure 3-5). As shown in Table 3-3, this watershed has around 17 percent developed land, with the other 27 percent consisting mostly of evergreen and mixed forest. The most common land cover in the watershed is woody wetlands with 32.5 percent of total area.

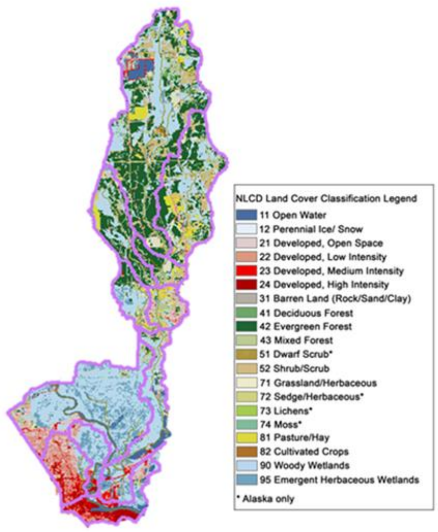

Figure 3-5. Illustration of the NLCD Land Cover Classification within the Neches River watershed.

Table 3-3. Land Cover summary of Neches River watershed.

Land Cover	**Acres**	**Percent of Total**
Woody Wetlands	16,546	32.5
Evergreen Forest	10,770	21.1
Emergent Herbaceous Wetlands	3,508	6.9
Developed, Open Space	3,177	6.2
Mixed Forest	3,081	6
Developed, Low Intensity	3,061	6
Shrub/ Scrub	2,819	5.5
Open Water	2,125	4.2
Hay/Pasture	1,659	3.3
Herbaceous	1,427	2.8
Developed, Medium Intensity	1,223	2.4
Developed, High Intensity	1,134	2.2
Barren Land	212	0.4
Deciduous Forest	123	0.2
Cultivated Crops	79	0.2
Total	50,943	100

3.4.3 Infiltration

Stormwater runoff is dispersed among two types of storage: infiltration (which serves as input to the groundwater compartment) and surface runoff. By estimating infiltration and subtracting those values from the total precipitation, the SWMM model replicates the process of surface runoff generation and its effects on the environment. As a result, infiltration modeling is a critical step in the simulation of stormwater runoff. SWMM has three ways for calculating infiltration: the Horton, Curve Number, and Green-Ampt approaches.. Curve Number infiltration strategy is selected and briefly covered in the following section. In addition, the curve number method is chosen to describe the relationship between infiltration rate and time. In this study, eleven catchments have been considered, and SWMM treats each catchment as a nonlinear reservoir considering the continuity and Manning's equations on each of them (Rossman, 2010)

The Curve Number method is the infiltration method used in TR-20/55 models. TR-20 model is applied for small watersheds in urban hydrology to estimate runoff curve number. Also, TR-55 model is a computer model for project formulation and hydrology which is applied to estimate runoff curve number. There is a report for TR-55 which is used in this study. Since curve number method is one of the most often used infiltration modeling methods, many resources such as TR-55 report, are available online for computing curve numbers. First, the percentages of different land cover types of are obtained for each catchment within the watershed using GIS. Then, considering the curve number values obtained from the descriptions of curve numbers from TR-55, a curve number value is assigned to each land cover type. Finally, an average value of curve number is ascribed for each catchment. .

3.4.4 Channel Flow Routing

There are three layers of modeling within the flow routing section of the model: steady flow routing, kinematic wave routing, and dynamic wave routing (James & Ferguson, 2020). When dealing with circular conduits, all three of these flow routing equations use the Hazen-Williams equation, and for all other conduit forms, Manning's Equation is used.

Steady routing is the most straightforward method, and it is based on a uniform distribution at each time step. Thus, hydrographs from upstream are translated downstream without attenuation, and channel storage or backwater effects are not considered (James & Ferguson, 2020). This option may be acceptable for long-term continuous simulation; however, this analysis is modeling fluctuations in inflow and precipitation during brief storm occurrences. Therefore, steady routing is not chosen in this case. The kinematic wave technique models track the flow downstream by employing the continuity equation and the momentum equation. It is only possible to model excess water as a loss to the system or a pond at the node from which water can be channeled. Backwater effects are not taken into consideration by the kinematic wave approach.

The Saint-Venant Equation may be solved completely using the dynamic wave approach, allowing for modeling pressured flow and backwater effects (James & Ferguson, 2020). When water levels at nodes and flow in conduits are combined, dynamic wave routing is a powerful solution used in virtually any type of system. Specifically, the system with considerable backwater effects due to downstream flow constraints and flow management provided by weirs and orifices are the greatest candidates for this technology. The kinematic wave technique for flow routing is selected due to the necessity for illustration of routing dynamics within a storm event without considering the flow's dynamic routing capabilities.

3.5 SWMM Model Parameter Description

It is necessary to define the sub-catchment land surface, junction/conduit, and rain gauge features once the modeling techniques for infiltration and flow routing have been determined and the sub-catchments have been established. This section describes the computational process of physical characteristics of each catchment's land surface properties, slope, width, surface roughness coefficient.

3.5.1 Sub-catchment Land Surface Properties

Sub-catchment properties were entered into the dialogue box using the following parameters: area, slope, width, percent impervious surface, Manning's roughness coefficient (n) for impervious and pervious surfaces, and percent impervious surface. Additionally, infiltration method parameters were entered into sub-catchments characteristics, and these parameters were then examined and estimated in ArcGIS. For example, the following parameters were computed for Curve Number infiltration: the curve number, saturated hydraulic conductivity, suction head, and starting deficit.

3.5.2 Slope Calculations

The analysis of elevation changes of the region, which impacts the rate and path of precipitation-runoff, was carried out using Digital Elevation Model (DEM) maps of the region. There are raster datasets in the map, and they reflect the surface elevation across the entire area, including depths below sea level. First, the average slope for the study region was estimated, measuring the elevation change from the inlet to the outflow and dividing it by the horizontal distance between the inlet and the outlet points. Eleven measurements were made, representing a nominal range of elevation fluctuations within the research region. Based on the digital elevation map (DEM) of the area of interest and application of the equation (3-1), the slope value for all catchments was calculated to roughly 3%.

Slope (%) = $\left(\frac{H}{d}\right) * 100$; where H = elevation (ft) and d = distance (ft) (3-1)

3.5.3 Width Calculations

For each sub-catchment, the width of the sub-catchment was estimated by measuring the length of an overland flow path using the DEM map in ArcGIS. According to the manual, the width of a sub-catchment is computed by dividing the area of each sub-catchment by the length of the overland flow, as shown in equation (3-2).

Width (%) = $\left(\frac{A}{D_{OF}}\right)$; where A = area (ft^2) and D_{OF} = Longest overland flow length (ft) (3-2)

For this equation, the longest flow path was computed for each sub-catchment.

3.5.4 Impervious Surfaces Roughness Coefficient

The percentage of impervious surfaces in each sub-catchment within the study region was calculated using a GIS database. For each of the 11 sub-catchments, the impervious area was divided by total area using ArcGIS to calculate the percent impervious area. The Manning's roughness coefficient values for impervious surfaces were obtained from the analysis of the test catchment (highlighted in green in Figure 3-2), which provides a range of values. The average value of the calculated range is chosen to represent the impervious “n” for each sub-catchment. Table 3-4 shows the results of the calculations for the sub-catchment parameters.

Table 3-4. Overland Flow Calculations

Catchment	Area (mi^2)	Flow length (mi.)	Width (ft)	Curve Number	Imperviousness
catchment 1	23.31	11.81	1.97	85	1.77
catchment 2	10.87	5.13	2.12	84	1.37
catchment 3	5.35	6.00	0.89	84	0.69
catchment 4	2.08	2.78	0.75	81	2.07
catchment 5	2.39	2.10	1.14	83	7.89
catchment 6	2.87	6.000	0.47	88	1.32
catchment 7	7.15	9.84	0.73	95	6.07
catchment 8	15.4	6.00	2.56	96	0.21
catchment 9	2.368	2.72	0.98	88	39.7
catchment 10	3.91	2.3	1.70	73	9.17
catchment 11	3.92	2.66	1.47	94	38.92

3.6 Best Management Practice (BMP) Implementation

In SWMM, the BMP module is a decentralized small-scale measure module integrated into the overall system. BMPs are environmentally friendly, simple to construct, compact in size, cost-effective, and ornamental landscape, among other characteristics. Although the BMP implementation process is considered to follow a decentralized mechanism in the real application, this study merges the sub-volumes of all smaller detention ponds into one individual larger BMP module. The main reason is that I tried to divide the catchments into smaller sub-catchments and consider a wet detention pond for each sub-catchment in SWMM. I compare the result of this process with the scenario that I have already considered in this study. This comparison shows the same result.

”The SWMM estimates the input and outflow of the subarea in real-time using the notion of water balance as a foundation. In this research, three BMP scenarios are implemented in SWMM to compare their runoff under various precipitation patterns.

This study designs BMP structures in the SWMM model (e.g., wet detention ponds) to control the storage capacity and, thus, manage the runoff quantity and quality attributes. This structure is deployed to reduce downstream flood hazards by temporarily retaining stormwater in the basin and slowly releasing it through outflow control structures (e.g., orifices in this study) over an extended period. For each storage unit, a tabular depth-area storage curve is introduced to the model. This study applied the trapezoid-shaped ponds with a 3:1 side slope and a maximum depth of 12 feet. It should be noted that pond volumes have been adjusted between the different design storms to achieve approximately 40% flow reduction in each catchment.

3.7 Design **Storm Approach**

Generally, the design storm is based mostly on the concept of the probability distribution. It is developed by analyzing the intensity-duration-frequency (IDF) curves or other statistical measures derived from precipitation data. When it comes to producing a reasonable design storm, the alternating block method, instantaneous intensity method, and triangular hyetograph method are the most commonly employed methods (Te Chow, 2010). In addition, it is common practice to combine the design storm method with the rational formula or a unit hydrograph approach to simulate the design flood hydrograph for water resources planning. On the other hand, these approaches do not account for the storage carryover effect that may occur in a drainage system due to the time interval between storms (Te Chow, 2010).

An alternating block method is a straightforward approach to creating a design storm from an IDF curve provided in NOAA's Atlas 14 for different average recurrence intervals. The design storm created by this approach specifies the precipitation depth in "n" consecutive time intervals of duration (t) over a total period. The precipitation intensity is retrieved from the IDF curve for each duration based on the design return period (Butler and John, 2011). Changing regional climate in the future may raise the flood risk of urban catchment areas, perhaps leading to floods during more frequent and severe storms. Therefore, it is vital to test a series of design storms, including severe ones, to examine runoff quantity management's capability and ensure that it can resist storms with longer return periods and last for extended periods. Gridded precipitation frequency estimates are provided by Atlas-14 using point-based gridded data (PFEs). First, to apply the alternating block method on PDS-based precipitation frequency estimates with 90% confidence intervals provided by NOAA ATLAS 14, different average recurrence intervals of 10, 25, 50, 100, 200, 500, and 1000 years are considered for a location within the area of interest. Second, the incremental precipitation from cumulative precipitation is computed. Third, the highest incremental precipitation (maximum block) is chosen and place it in the middle of the hyetograph; then the second highest block is chosen and place it to the right of the maximum block, also the third highest block is selected and place it to the left of the maximum block, and so on until the last block. Accordingly, three design storms have been selected further to analyze BMPs implementation and cost-benefit analysis of these BMPs. Each is clustered by return period 25 years (25-yr), 50 years (50-yr), and 100 years (100-yr) and duration of 5 days. The goals are to evaluate the efficiency and cost-benefit of these BMPs on bacteria reduction in the Neches River watershed, which are based on the simulation results of the flow in the SWMM model.

3.8 Micro-Organism Prediction in Urban Stormwater (MOPUS) Model

McCarthy and colleagues developed the MOPUS model to simulate E. coli levels in stormwater catchments using a precipitation-runoff model and a micro-organism model. When impervious surfaces are simulated, the microbe model incorporates surface and subsurface components to simulate the buildup and washing from micro-organisms. Micro-organisms obtain their food from both animals and humans. The longevity of these microbes depends on various environmental conditions, including temperature, humidity, pH, nutrition content, salinity, and toxicity, once they have been deposited. The microbes are then moved, which is frequently accomplished by the occurrence of runoff. This analysis only considers surface storage to estimate bacteria concentration within each catchment. The governing equations for the micro-organism model are presented in Table 3-5. McCarthy et al., 2011 (McCarthy et al., 2011) provide a thorough introduction to MOPUS, shown in Table 3-5.

Table 3-5. The governing equations of the micro-organism model in MOPUS.

Model Equation	**Comment**
$P_s(t) = 10^{PsCoeff} \times \left[\frac{VP(t-1)}{\overline{VP}}\right]^{VPCoeff} \times \left[\frac{RH(t-1)}{\overline{RH}}\right]^{RHCoeff}$	Surface storage
$C_s(t) = \frac{P_s(t) \times RI(t)^{1.293}}{RI(t)}$	Surface wash-off

where Ps(t) indicates the number of surface storage (of microorganisms), VP(t−1) is previous day's vapor pressure (hpa), $\overline{VP}$ is the mean VP(t) value (hpa), RH(t−1) represents previous day's maximum relative humidity (%), $\overline{RH}$ is the mean RH(t) value (%), PsCoeff, VPCoeff and RHCoeff are the calibration coefficients, $C_s(t)$ is the number of microorganisms which are removed from the surface storage through wash-off (orgs/L), and RI(t) is the routed and translated precipitation intensity (mm/min).

3.9 Development of the MOPUS_S Model

MOPUS_S is the name given to the semi-distributed model that was constructed in this work. The transition from MOPUS to MOPUS_S model is primarily comprised of three aspects: taking into account the effects of land-use types on microbial accumulation; coupling SWMM with MOPUS model in order to leverage the advantages of hydrological simulation; and changing the constant in MOPUS to a calibration parameter in MOPUS_S in order to complete the localization of parameters. The following were the specific algorithms used by MOPUS_S:

(1) Surface storage in a single sub-catchment

$$P_{si}(t) = 10^{P_{si}\,\mathrm{Coeff}} \times \left[\frac{VP(t-1)}{\overline{VP}}\right]^{\mathrm{VPCoeff}} \times \left[\frac{RH(t-1)}{\overline{RH}}\right]^{\mathrm{RHCoeff}} \times S_i \quad (\mathrm{orgs}) \tag{3-3}$$

where Psi(t) is the pollutant accumulated in the i^{th} sub-catchment area, in organisms; Si is the area of the i^{th} sub-catchment, in ha; P_{si} Coeff, VPCoeff, and RHCoeff are the calibration coefficients; VP (t-1) is the vapor pressure measured the previous day in hpa; $\overline{VP}$ is the mean vapor pressure measured current day in hpa; RH (t-1) is the maximum relative humidity measured the previous day in percent; RH (t-1) is the mean relative humidity measured the current day in percent. The wet-bulb temperature at 9 a.m. was used to determine the vapor pressure. At the same time, the relative humidity was taken from data acquired from the meteorological station, and S_i was extracted from the SWMM input.

(2) Surface wash-off in a single sub-catchment

$$C_{si}(t) = \frac{P_{si}(t) \times \left[\frac{6Q_i(t)}{S_i}\right]^{C_s\,\mathrm{Coeff}}}{6 \times 10^5 Q_i(t)} \quad (\mathrm{org}/100\ \mathrm{mL}) \tag{3-4}$$

where $Q_i(t)$ is the surface runoff of the i^{th} sub-catchment, calculated from the SWMM output (converted to mL/min), and the constants in the formula are for unit conversion. The final orgs/100 mL result corresponds to our monitoring measurement of the most probable number (MPN)/100 mL, which we obtained using a titration process. The calibration parameter is represented by the symbol C_s Coeff.

To estimate the bacteria concentration in five days of Hurricane Harvey, the meteorological characteristics from 08/26/2017 to 08/30/2017 are obtained from the National Solar Radiation Database website. The model input parameters, including temporal changes of relative humidity and vapor pressure values, are obtained from National Solar Radiation Database and National Oceanic and Atmospheric Administration (NOAA), respectively, as shown in Table 3-6.

Table 3-6. Hydrometeorological variables the period from 08/26/2017 to 08/30/2017.

	Relative humidity of the current day	Relative humidity of the previous day	Average vapor pressure of current day (hPa)	Vapor pressure of previous day (hPa)
08/26/2017	99	98	33.25	31.31
08/27/2017	100	99	32.1	33.25
08/28/2017	99	100	31.55	32.1
08/29/2017	98	99	27.21	31.55
08/30/2017	97	98	25.35	27.21

3.10 Calibration Process of MOPUS_S Model

The calibration process of flow for the Neches River watershed could not be conducted since no USGS flow gauging station is located downstream of the eleven catchments and the tributaries of the Neches River watershed. However, there is a TCEQ station number 10575, located near the downstream of the watershed, that reported the average concentration of bacteria on 1/14/2016 and 7/19/2016. The average bacteria concentration is reported 150 and 610 (organisms) for these two dates, respectively.

3.11 Cost-Benefit Analysis

As a decision-making tool for BMP strategies, cost-benefit analysis is concerned with the proper hydro-performance of the BMP procedures that are being examined. It is used to evaluate the runoff management performance of a BMP design in terms of peak flow and runoff volume reduction to the construction expenses connected with that technique. Here, three scenarios are defined to conduct cost-effectiveness and cost-benefit analyses of detention pond implementation in controlling non-point source pollution in the Neches River watershed. For further information, the readers are suggested to refer to sections 4.3 and 4.5.

4. RESULTS

4.1 Different Design Storms

In this work, the design storm at a single rain gauge was structured using the alternating block approach derived from the intensity-duration-frequency (IDF) curve distribution. Figure 4-1 depicts the seven synthetic hyetographs for average recurrence intervals of 10 years (ARI-10), 25 years (ARI-25), 50 years (ARI-50), 100 years (ARI-100), 200 years (ARI-200), 500 years (ARI-500), and 1000 years (ARI-1000) that resulted from the alternating Block approach; all of the storms are specified with a time interval of 60 minutes and a total length of 5 days. The alternating block pattern catches an individual peak, and the time to peak is set at 3660 minutes, which occurs on the third day of a five-day period. The design storms for different return periods show the same pattern; however, the peak intensity gets higher for higher average recurrence intervals. The range of the peak values falls between 3.25 and 6.85 inches per hour for the average recurrence intervals ranging between 10 and 1000 years.

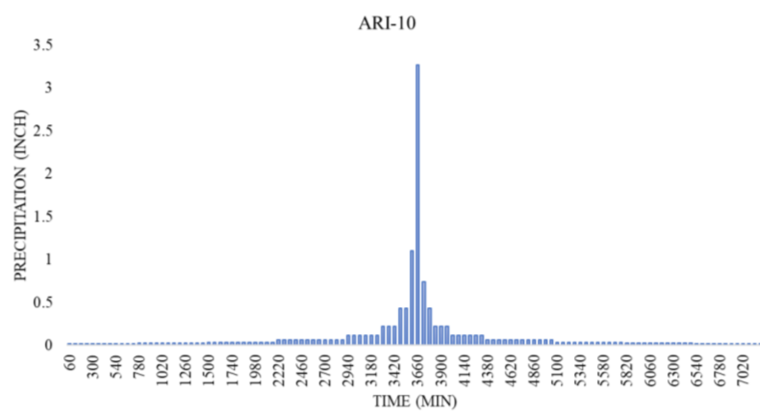

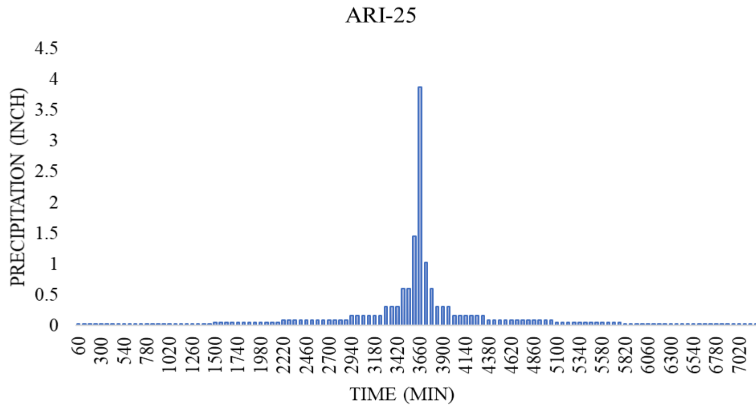
ARI-25
4.5
4
3.5
3
2.5
2
1.5
1
0.5
0
PRECIPITATION (INCH)
60
300
540
780
1020
1260
1500
1740
1980
2220
2460
2700
2940
3180
3420
3660
3900
4140
4380
4620
4860
5100
5340
5580
5820
6060
6300
6540
6780
7020
TIME (MIN)

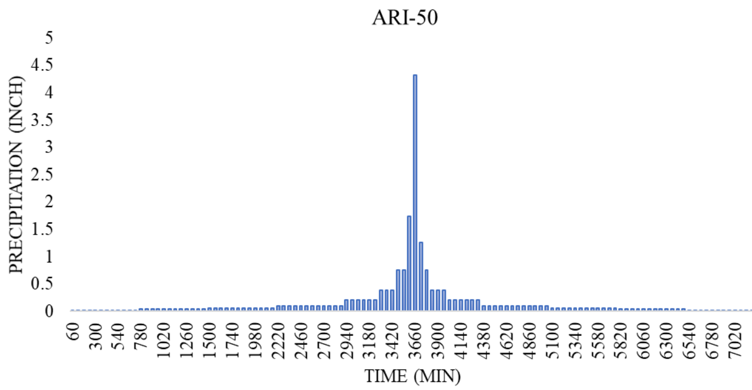
ARI-50
5
4.5
4
3.5
3
2.5
2
1.5
1
0.5
0
PRECIPITATION (INCH)
60
300
540
780
1020
1260
1500
1740
1980
2220
2460
2700
2940
3180
3420
3660
3900
4140
4380
4620
4860
5100
5340
5580
5820
6060
6300
6540
6780
7020
TIME (MIN)

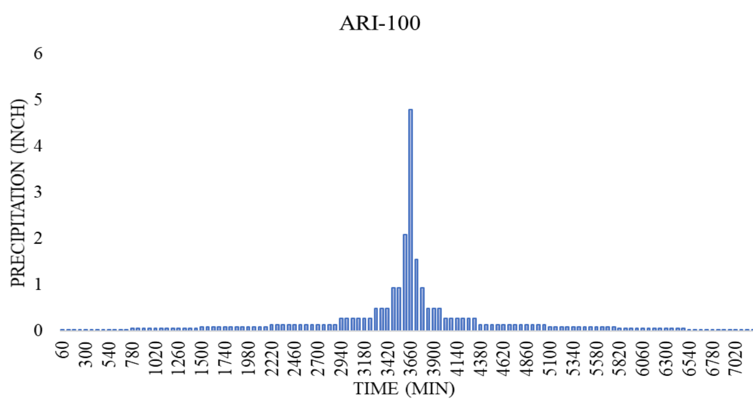
ARI-100
6
5
4
3
2
1
0
PRECIPITATION (INCH)
60
300
540
780
1020
1260
1500
1740
1980
2220
2460
2700
2940
3180
3420
3660
3900
4140
4380
4620
4860
5100
5340
5580
5820
6060
6300
6540
6780
7020
TIME (MIN)

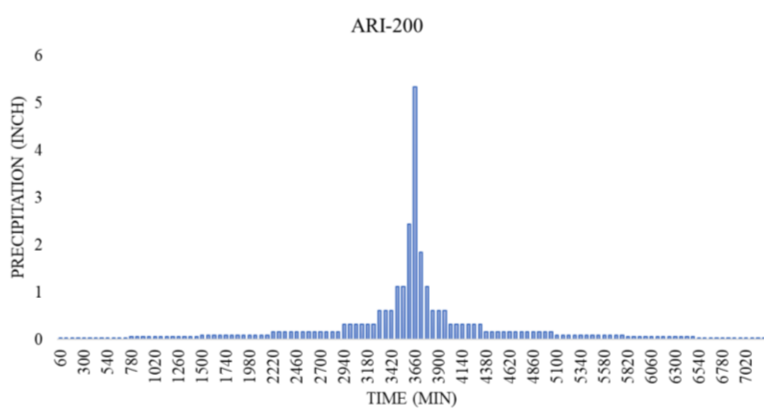
ARI-200
6
5
4
3
2
1
0
PRECIPITATION (INCH)
60
300
540
780
1020
1260
1500
1740
1980
2220
2460
2700
2940
3180
3420
3660
3900
4140
4380
4620
4860
5100
5340
5580
5820
6060
6300
6540
6780
7020
TIME (MIN)

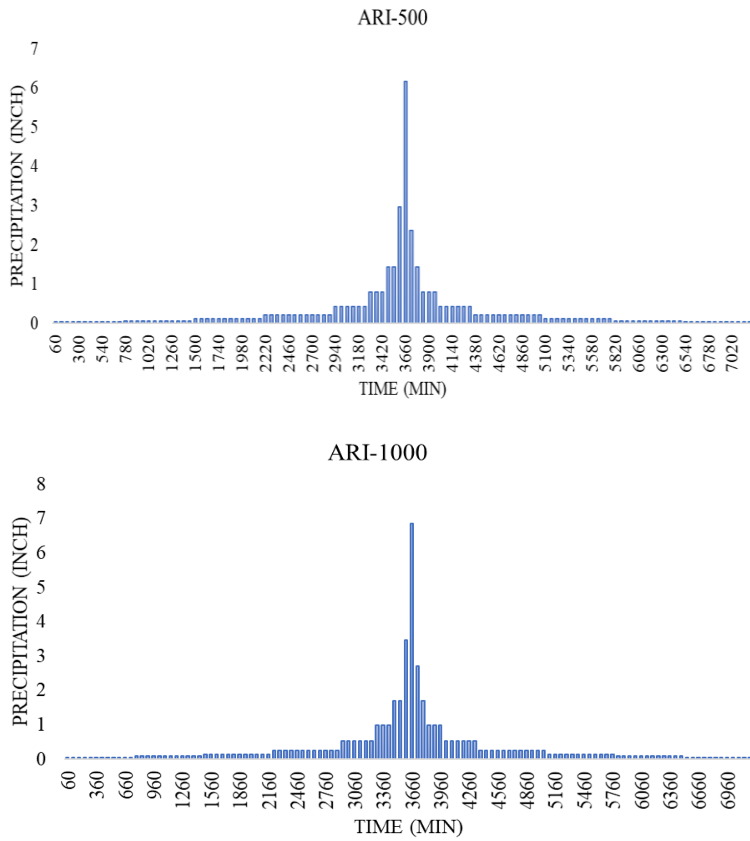

Figure 4-1. Hyetographs of different average recurrence intervals.

4.2 SWMM model calibration

Since there is no streamflow station downstream and within the tributaries of the Neches River watershed, the calibration process is conducted for a surrogate catchment considered as a test watershed. The physical component of this catchment in SWMM is shown in Table 4-1. Calibration is conducted for the time intervals of 10/1/2002 to 10/31/2002, 3/1/2016 to 3/31/2016, and 4/1/2016 to 4/30/16.

Comparing the observation flow resulting from the SWMM for these intervals, the values of manning's n have been calculated for overland flow on both pervious and impervious sections of this surrogate watershed. The average manning’s values of the previous and impervious areas are estimated at 0.2 and 0.07, respectively.

Table 4-1. Physical characteristics of the surrogate watershed in SWMM.

Physical characteristics in SWMM	Value
Area (ha)	23050
Width (m)	500
Slope (%)	2
Imperviousness	50
Curve Number	80

Figure 4-2 illustrates the observed and simulated flow comparison to obtain the manning's roughness coefficient for pervious and impervious surfaces for three proposed time intervals.

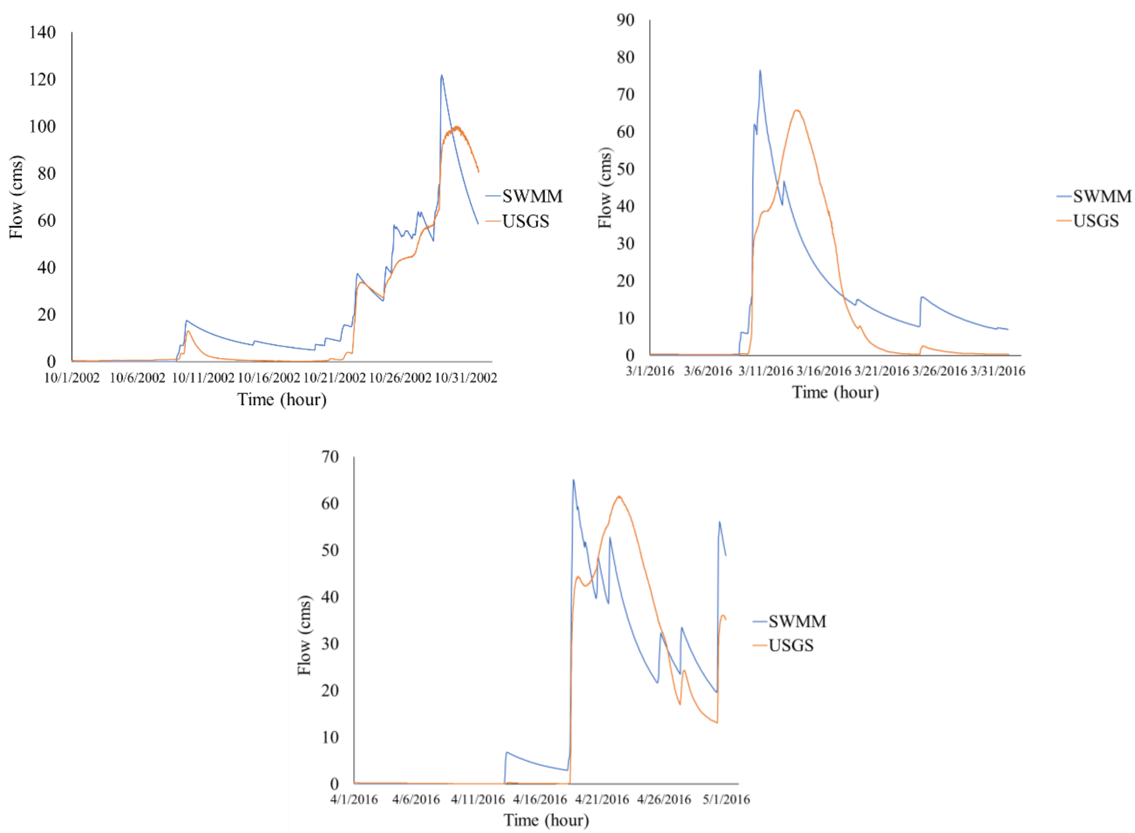

Figure 4-2. Simulated and observed flow in the test catchment within three proposed time intervals.

4.3 Defined scenarios for BMPs implementation in SWMM

In Figure 4-3, three scenarios are defined to conduct cost-effectiveness and cost-benefit analyses of detention pond implementation in controlling non-point source pollution in the Neches River watershed. Scenario 1 outlines the application of detention ponds in three catchments of 2, 5, and 7, shown in Figure 4-3 (a). Scenario 2 defines the application of detention ponds in five catchments of 2, 4, 5, 7, and 11, shown in Figure 4-3 (b). Lastly, scenario 3 specifies the application of detention ponds in seven catchments of 1, 2, 4, 5, 6, 7, and 11, shown in Figure 4-3 (c). The criterion for selecting these catchments is based on the density of on-site sewage facilities (OSSFs) located in each catchment compared to its counterparts with lower OSSF density. It should be mentioned that the malfunctioning and demolishing of these facilities at the time of flooding is a primary reason for selected catchments as they are prone to be contaminated with high concentrations of bacteria produced by failed OSSFs.

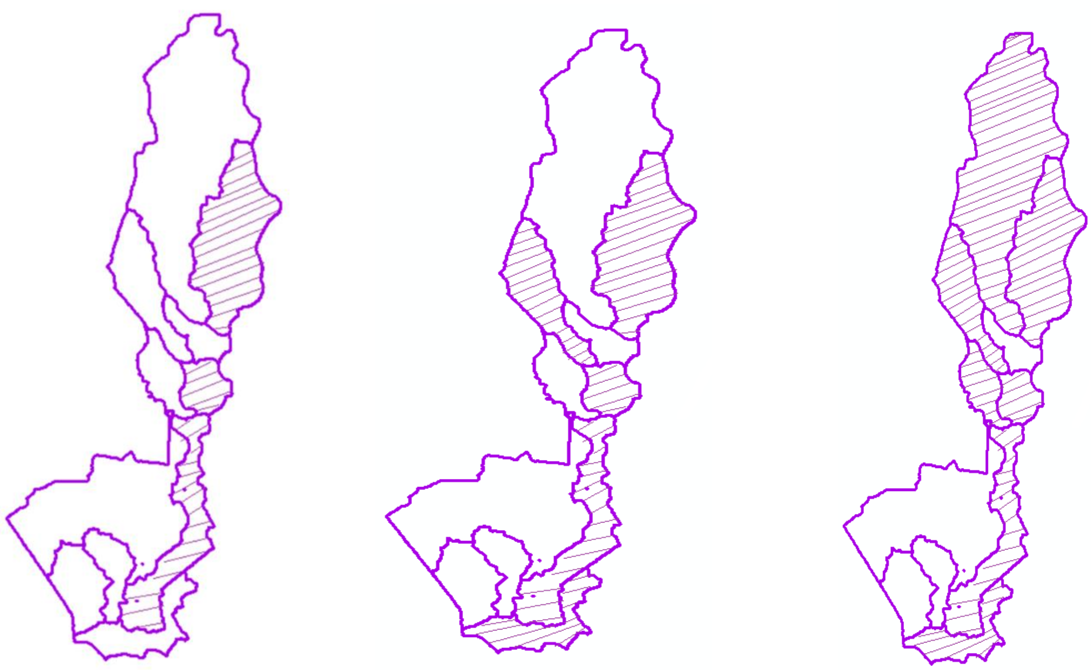

(a) First Scenario (b) Second Scenario (c) Third Scenario

Figure 4-3. Illustration of three scenarios and their included catchments.

Table 4-2 indicates the percentages of detention ponds that have been considered for the 25-yr, 50-yr, and 100-yr design storms.

Table 4-2. Wet detention ponds implementation percentage in the catchments in response to various design storms.

Catchment	Area (mi^2)	25-yr		50-yr		100-yr	
		Pond Area (mi^2)	Pond Area Percentage (%)	Pond Area (mi^2)	Pond Area Percentage (%)	Pond Area (mi^2)	Pond Area Percentage (%)
1	16.44	0.23	1.4	0.35	2.13	0.4	2.5
2	5.15	0.1	2	0.14	2.7	0.2	4
4	4.08	0.09	2.2	0.14	3.5	0.17	4.2
5	2.39	0.07	3	0.08	3.3	0.1	4.2
6	2.87	0.08	2.8	0.12	4.2	0.15	5.2
7	7.15	0.17	2.4	0.22	3	0.3	4.2
11	3.92	0.09	2.3	0.12	3	0.15	4

4.4 Water Quantity Reduction Using BMP

To limit peak runoff, it was necessary to apportion surface runoff from the catchments and store it in BMP facilities. The drainage capacity of BMP techniques, however, may be quickly surpassed during high-intensity design storms. Therefore, to prevent bypass runoff, the size of BMPs increases for higher design storms. Table 4-3 illustrates the performance of BMPs for mitigation of the peak flow under various design storms. Figure 4-4 – 5-6 illustrates the application of detention ponds in catchments 1, 2, 4, 5, 6, 7, and 11. Considering design storms of 25-yr, 50-yr, and 100-yr, illustrated in Figure 4-4 – 5-6, show that the application of detentions ponds implies an approximate reduction of the peak flow of approximately 40% in these catchments. Additionally, it can be deduced from Figure 4-4 – 5-6 that peak flow rate reduction is successful in higher design storms only if higher volumes of BMP infrastructures are used.

Table 4-3. Peak flow reduction after BMPs implementation in the catchments for 25-yr, 50-yr, and 100-yr design storms.

Catchment	25-yr		50-yr		100-yr	
	Peak Flow before BMP (cfs)	Peak Flow after BMP (cfs)	Peak Flow before BMP (cfs)	Peak Flow after BMP (cfs)	Peak Flow before BMP (cfs)	Peak Flow after BMP (cfs)
1	202	130	265	170	338	220
2	102	62	130	70	162	89
4	72	39	91	48	105	58
5	59	37	74	43	90	49
6	39	24	50	27	60	32
7	77	47	99	57	126	72
11	112	66	130	70	150	80

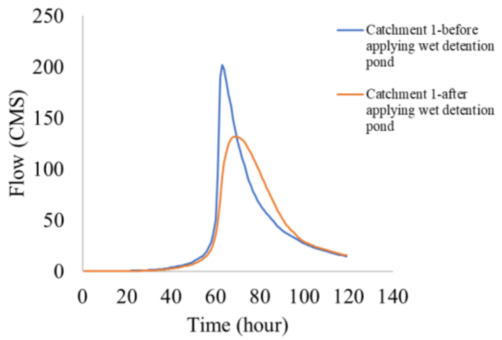
Flow (CMS)
Time (hour)
Catchment 1-before applying wet detention pond
Catchment 1-after applying wet detention pond

(a)

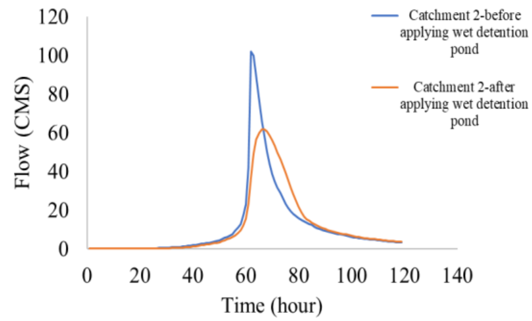
Flow (CMS)
Time (hour)
Catchment 2-before applying wet detention pond
Catchment 2-after applying wet detention pond

(b)

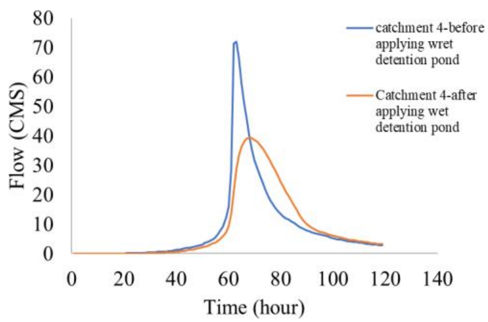
Flow (CMS)
Time (hour)
catchment 4-before applying wret detention pond
Catchment 4-after applying wet detention pond

(c)

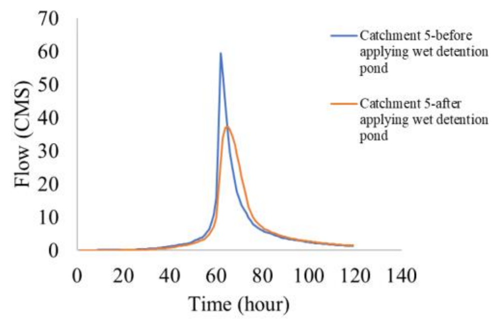
Flow (CMS)
Time (hour)
Catchment 5-before applying wet detention pond
Catchment 5-after applying wet detention pond

(d)

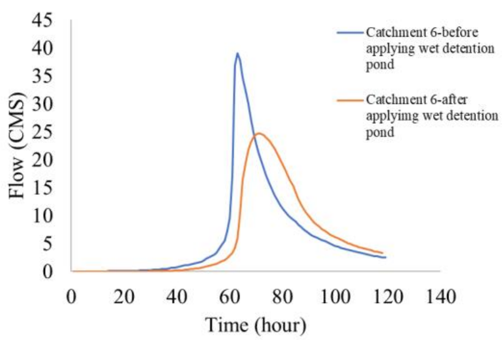
Flow (CMS)
Time (hour)
Catchment 6-before applying wet detention pond
Catchment 6-after applyimg wet detention pond

(e)

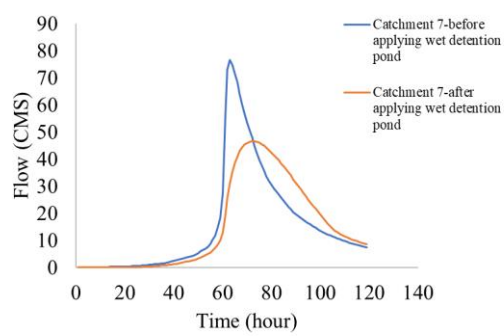
Flow (CMS)
Time (hour)
Catchment 7-before applying wet detention pond
Catchment 7-after applying wet detention pond

(f)

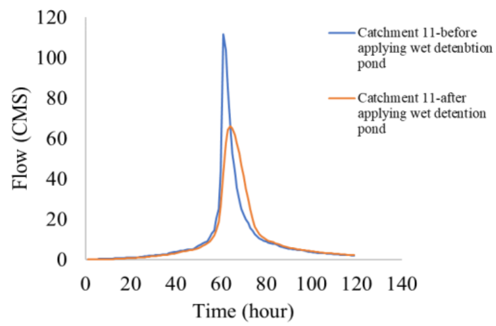

(g)

Figure 4-4. Illustration of three scenarios considering 25-yr design storm. Flow time series before and after applying wet detention ponds in the catchments (a) catchment 1, (b) catchment 2, (c) catchment 4, and (d) catchment 5, (e) catchment 6, (f) catchment 7, (g) catchment 11.

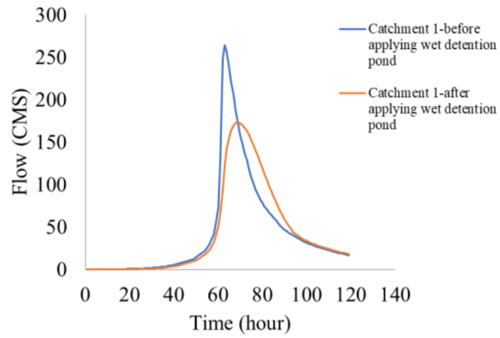
Catchment 1-before applying wet detention pond
Catchment 1-after applying wet detention pond
Flow (CMS)
Time (hour)

(a)

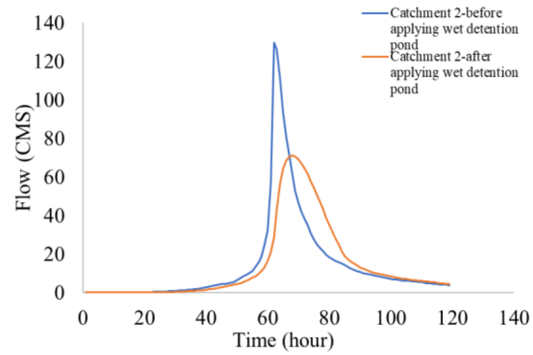
Catchment 2-before applying wet detention pond
Catchment 2-after applying wet detention pond
Flow (CMS)
Time (hour)

(b)

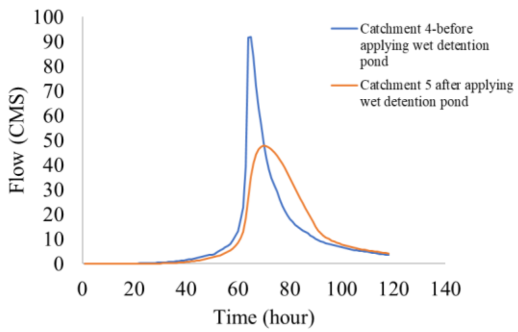
Catchment 4-before applying wet detention pond
Catchment 5 after applying wet detention pond
Flow (CMS)
Time (hour)

(c)

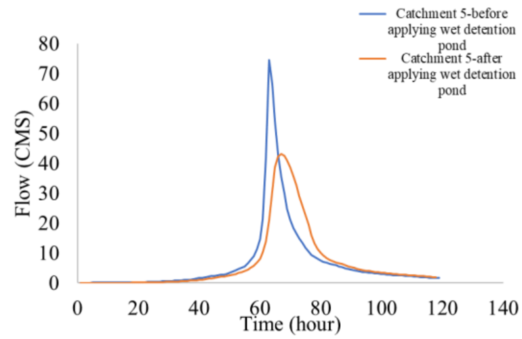
Catchment 5-before applying wet detention pond
Catchment 5-after applying wet detention pond
Flow (CMS)
Time (hour)

(d)

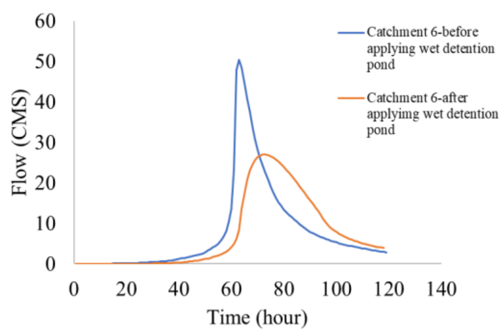
Catchment 6-before applying wet detention pond
Catchment 6-after applying wet detention pond
Flow (CMS)
Time (hour)

(e)

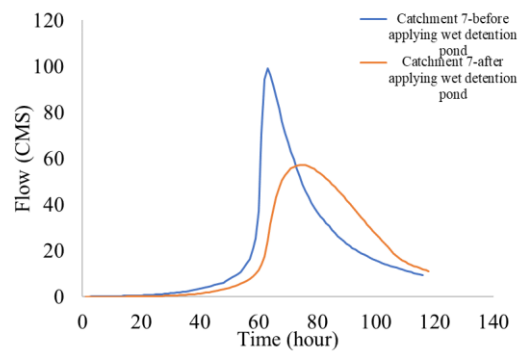
Catchment 7-before applying wet detention pond
Catchment 7-after applying wet detention pond
Flow (CMS)
Time (hour)

(f)

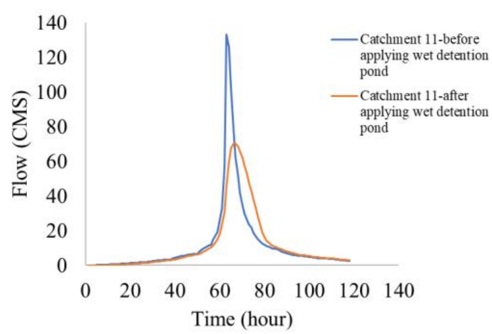
Catchment 11-before applying wet detention pond
Catchment 11-after applying wet detention pond
Flow (CMS)
Time (hour)

(g)

Figure 4-5. Illustration of three scenarios considering 50-yr design storm. Flow time series before and after applying wet detention ponds in the catchments (a) catchment 1, (b) catchment 2, (c) catchment 4, and (d) catchment 5, (e) catchment 6, (f) catchment 7, (g) catchment 11.

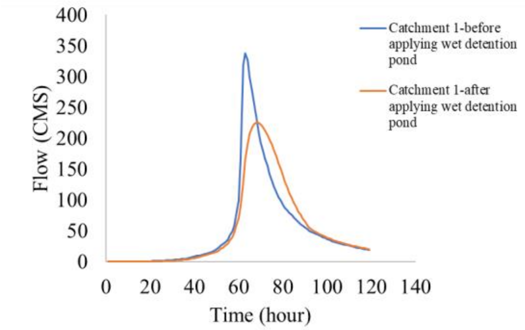
Flow (CMS)
Time (hour)
Catchment 1-before applying wet detention pond
Catchment 1-after applying wet detention pond

(a)

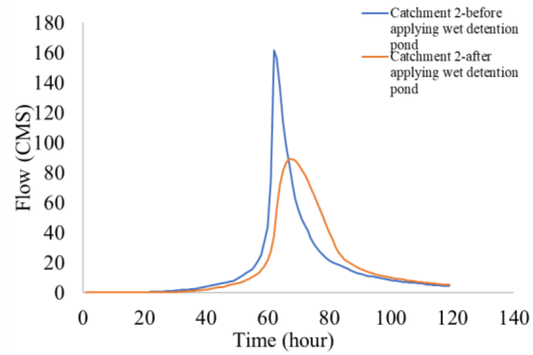
Flow (CMS)
Time (hour)
Catchment 2-before applying wet detention pond
Catchment 2-after applying wet detention pond

(b)

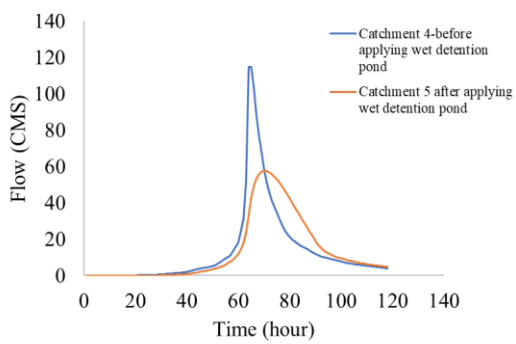
Flow (CMS)
Time (hour)
Catchment 4-before applying wet detention pond
Catchment 5 after applying wet detention pond

(c)

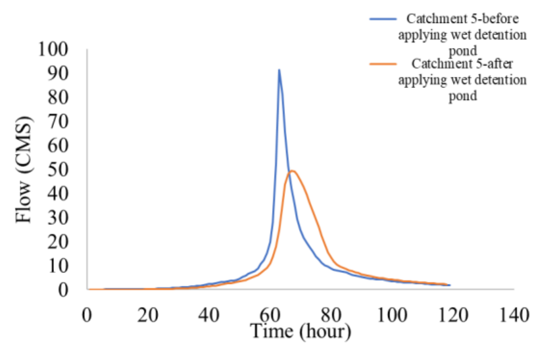
Flow (CMS)
Time (hour)
Catchment 5-before applying wet detention pond
Catchment 5-after applying wet detention pond

(d)

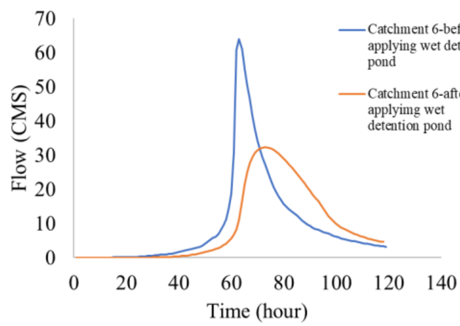
Flow (CMS)
Time (hour)
Catchment 6-before applying wet detention pond
Catchment 6-after applyimg wet detention pond

(e)

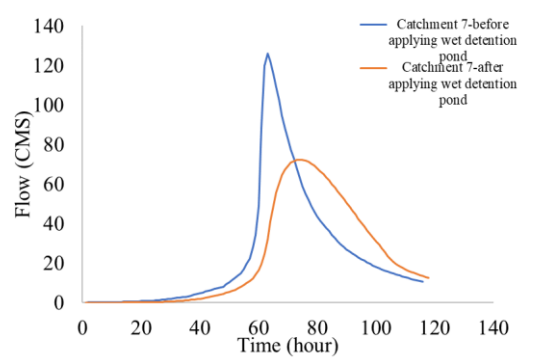
Flow (CMS)
Time (hour)
Catchment 7-before applying wet detention pond
Catchment 7-after applying wet detention pond

(f)

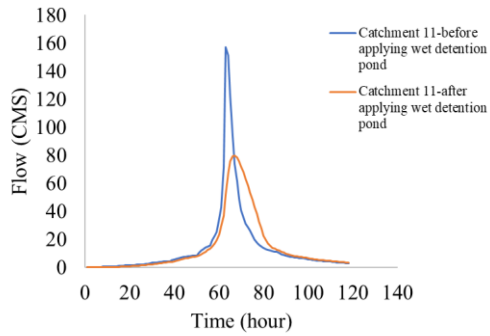

(g)

Figure 4-6. Illustration of three scenarios considering 100-yr design storm. Flow time series before and after applying wet detention ponds in the catchments (a) catchment 1, (b) catchment 2, (c) catchment 4, and (d) catchment 5, (e) catchment 6, (f) catchment 7, (g) catchment 11.

4.5 Cost-benefit analysis

As a decision-making tool for BMP strategies, cost-benefit analysis relates to the appropriate hydro-performance of the BMP techniques being considered. It is used to compare the runoff management performance of a BMP plan in terms of peak flow and runoff volume reduction versus the construction costs associated with that approach. As the population of OSSFs is congested in certain regions of the catchments, this study only considers these regions and their associated area for detention pond design and analysis. The construction cost of detention ponds is calculated using the EPA's empirical approach: cost is considered to be equal to 33.55 $V^{0.705,}$ where V is the detention pond volume (ft^3). In the original equation, the construction cost of a wet detention pond was created in 1997 and is adjusted for inflation. Table 4-4 – 4-6 indicate the cost-benefit analysis results for the defined three scenarios in 25-yr, 50-yr, and 100-yr design storms. These cost-benefit analyses can be used to assist decision-makers in identifying appropriate BMP solutions that are compatible with a variety of financial restrictions and environmental implications in response to anticipated climate change scenarios. Our findings demonstrate that the cost of BMP construction for the three scenarios under 25-yr design storm is $17M, $27M, $40.5M; for the three scenarios under 50-yr design storm are $22M, $35M, $52M; and for the three scenarios under 100-yr design storm are $25M, $40M, $59M. Depending on the priority selection of scenarios for decision-makers and availability of rehabilitation budget, each of these scenarios can be of interest for the stormwater management programs to mitigate the adverse impacts of flooding, including peak flow and runoff volume.

Table 4-4. Three scenarios of detention pond application and associated cost estimation and maximum flow reductions considering 25-year design storm.

First Scenario							
Catchment	Catchment Area (mi^2)	Pond Area (mi^2)	Pond Area Percentage (%)	Maximum Depth (ft)	Volume (Ac-ft)	Cost ($M)	Maximum flow reduction (%)
Catchment 2	5.15	0.1	2	12	717	5	40
catchment 5	2.39	0.07	3	12	529	4	38
catchment 7	7.15	0.17	2	12	1300	8	40
Total Cost ($ M)						**17**	
Second Scenario							
Catchment	Catchment Area (mi^2)	Pond Area (mi^2)	Pond Area Percentage (%)	Maximum Depth (ft)	Volume (Ac-ft)	Cost ($M)	Maximum flow reduction (%)
Catchment 2	5.15	0.1	2	12	717	5	40
catchment 4	4.08	0.09	2	12	669	5	43
catchment 5	2.39	0.07	3	12	529	4	38
catchment 7	7.15	0.17	2	12	1300	8	40
catchment 11	3.92	0.09	2	12	669	5	40
Total Cost ($ M)						**27**	
Third Secenario							
Catchment	Catchment Area (mi^2)	Pond Area (mi^2)	Pond Area Percentage (%)	Maximum Depth (ft)	Volume (Ac-ft)	Cost ($M)	Maximum flow reduction (%)
catchment 1	16.44	0.23	1.4	12	1500	9	35

Catchment 2	5.15	0.1	2	12	669	5	40
catchment 4	4.08	0.09	2.2	12	669	5	43
catchmen 5	2.39	0.07	3	12	529	4	38
catchment 6	2.87	0.08	2.8	12	571	4.5	35
catchment 7	7.15	0.17	2.4	12	1300	8	40
catchment 11	3.92	0.09	2.3	12	669	5	40
Total Cost ($ M)						**40.5**	

Table 4-5. Three scenarios of detention pond application and associated cost estimation and maximum flow reductions considering 50-yr design storm.

Catchment	Catchment Area (mi^2)	Pond Area (mi^2)	Pond Area Percentage (%)	Maximum Depth (ft)	Volume (Ac-ft)	Cost ($M)	Maximum flow reduction (%)
First Scenario							
Catchment 2	5.15	0.14	2.7	12	984	7	46
catchment 5	2.39	0.08	3.5	12	555	5	44
catchment 7	7.15	0.22	3	12	1644	10	42
Total Cost ($M)						**22**	
Second Scenario							
Catchment	Catchment Area (mi^2)	Pond Area (mi^2)	Pond Area Percentage (%)	Maximum Depth (ft)	Volume (Ac-ft)	Cost ($M)	Maximum flow reduction (%)
Catchment 2	5.15	0.14	2.7	12	984	7	46
catchment 4	4.08	0.14	3.5	12	984	7	45
catchment 5	2.39	0.08	3.5	12	555	5	44
catchment 7	7.15	0.22	3	12	1644	10	42
catchment 11	3.92	0.09	2	12	840	6	45
Total Cost ($M)						**35**	
Third Scenario							
Catchment	Catchment Area (mi^2)	Pond Area (mi^2)	Pond Area Percentage (%)	Maximum Depth (ft)	Volume (Ac-ft)	Cost ($M)	Maximum flow reduction (%)
catchment 1	16.44	0.35	2.5	12	1990	11	35

Catchment 2	5.15	0.14	2.7	12	984	7	46
catchment 4	4.08	0.14	3.5	12	984	7	45
catchment 5	2.39	0.08	3.3	12	555	5	44
catchment 6	2.87	0.12	4.2	12	840	6	44
catchment 7	7.15	0.22	3	12	1644	10	42
catchment 11	3.92	0.12	3	12	840	6	45
Total Cost ($M)						**52**	

Table 4-6. Three scenarios of detention pond application and associated cost estimation and maximum flow reductions considering 100-yr design storm.

Catchment	Catchment Area (mi^2)	Pond Area (mi^2)	Pond Area Percentage (%)	Maximum Depth (ft)	Volume (Ac-ft)	Cost ($M)	Maximum flow reduction (%)
First Scenario							
Catchment 2	5.15	0.2	4	12	1558	9	44
catchment 5	2.39	0.1	4.2	12	698	5	44
catchment 7	7.15	0.3	4.2	12	1990	11	44
Total Cost ($ M)						**25**	-
Second Scenario							
catchment 2	5.15	0.2	4	12	1558	9	44
catchment 4	4.08	0.14	3.5	12	1270	8	44
catchment 5	2.39	0.1	4.2	12	698	5	44
catchment 7	7.15	0.3	4.2	12	1990	11	44
catchment 11	3.92	0.15	2	12	1127	7	45
Total Cost ($ M)						**40**	
Third Scenario							
catchment 1	16.44	0.4	2.5	12	2710	13	40

catchment 2	5.15	0.2	4	12	1558	9	44
catchment 4	4.08	0.17	4.2	12	1270	8	44
catchment 5	2.39	0.1	4.2	12	698	5	44
catchment 6	2.87	0.15	5.2	12	1127	6	44
catchment 7	7.15	0.3	4.2	12	1990	11	44
catchment 11	3.92	0.15	4	12	1127	7	45
Total Cost ($ M)						**59**	

4.6 Water Quality Improvement Using BMP

Using these bacteria concentrations, the MOPU_S model has been calibrated with the favorable coefficients listed in Table 4-7. The average value of $P_{siCoeff}$ is 7.82, and it is considered for further bacteria concentration calculation.

Table 4-7. Values of the calibrated parameters for the MOPUS_S model.

Report date: 01/14/2016			
P_{si}Coeff	VP Coeff	RH Coeff	C_sCoeff
7.7	2	2	2
Report date: 07/19/2016			
P_{si}Coeff	VP Coeff	RH Coeff	C_sCoeff
7.94	2	2	2

The bacteria growth and die-off rates strongly depend on the temporal variability of ambient relative humidity and vapor pressure variables. The estimated Bacteria concentration varies significantly across various catchments due to the diverse physical qualities of the catchments and the different land-use types in the catchments. Table 4-8 – 9-10 summarizes the catchment's bacteria statistics assuming Hurricane Harvey as hypothetical 25-year, 50-year, and 100-year design storms. The bacteria concentration is lowest in catchments 1 and 7, whereas it is highest in catchments 5 and 11. Additionally, the results indicate that the estimated bacteria concentrations result in higher values for 100-year design storms than 25-year and 50-year design storms. The peak of bacteria concentration is on the fourth day (08/29/2017), occurring one day after the peak flow estimated by the synthetic design storm. Given the catchment area and the associated peak flow, it is concluded that the bacteria concentration measurement is indirectly dependent on the nonlinear production of the catchment area and peak flow.

Table 4-8. Summary of statistics of bacteria concentration for 25-yr storm design

	First day (08/26/2017), Second day (08/27/2017), Third day (08/28/2017), Fourth day (08/29/2017), Fifth day (08/30/2017)		
	Bacteria Concentration (before BMPs)	Bacteria Concentration (After BMPs)	Percentage Reduction
Catchments 1	163.38/ 197.73 / 198.60 / 257.98/ 221.13	106.35/ 128.71/ 129.27/ 167.93/ 143.94	34.9
Catchments 2	263.01/318.32/319.71/ 415.31/355.98	159.11/192.57/193.41/ 251.25/215.35	39.5
Catchments 4	234.66/284.00/285.24/ 370.53/317.60	128.10/155.03/155.71/ 202.27/173.38	45.4
Catchments 5	330.75/400.30/402.05/ 522.28/447.66	208.39/252.21/253.31/ 329.06/282.05	58.7
Catchments 6	180.80/218.81/219.77/ 285.49/244.70	114.41/138.47/139.07/ 180.66/154.85	36.7
Catchments 7	142.63/172.62/173.38/ 225.23/193.05	86.70/104.93/105.38/ 136.90/117.34	39.2
Catchments 11	379.57/459.37/461.38/ 599.35/513.73	226.43/274.05/275.25/ 357.55/306.47	40.34

Table 4-9. Summary of statistics of bacteria concentration for 50-yr storm design

	First day (08/26/2017), Second day (08/27/2017), Third day (08/28/2017)., Fourth day (08/29/2017), Fifth day (08/30/2017)		
	Bacteria Concentration (before BMPs)	Bacteria Concentration (After BMPs)	Percentage Reduction
Catchments 1	213.74/ 258.68 / 259.81/ 337.50/ 289.28	140.18/ 169.65/ 170.40/ 221.35/ 189.73	34.4
Catchments 2	334.92 / 405.34 / 407.12 / 528.86 / 453.30	183.78 / 222.42 / 223.40/ 290.20 / 248.74	45.13
Catchments 4	299.37 / 362.32 / 363.91 / 472.73 / 405.19	156.12 / 188.95 / 189.78/ 246.53 / 211.31	47.85
Catchments 5	414.28/ 501.38/ 503.58/ 654.16/ 560.71	240.44/ 291.00/ 292.27/ 379.67/ 325.43	41.96
Catchments 6	233.69/ 282.83/ 284.07/ 369.01/ 316.29	124.94/ 151.20/ 151.87/ 197.28/ 169.10	46.54
Catchments 7	184.43/ 223.21/ 224.18/ 291.22/ 249.62	106.59/ 129.00/ 129.57/ 168.31/ 144.26	42.2
Catchments 11	452.46 / 547.60 / 549.99 / 714.46 / 612.39	239.17 / 289.46 /290.73/ 377.67 / 323.71	47.14

Table 4-10. Summary of statistics of bacteria concentration for 100-yr storm design.

	First day (08/26/2017), Second day (08/27/2017), Third day (08/28/2017), Fourth day (08/29/2017), Fifth day (08/30/2017)		
	Bacteria Concentration (before BMPs)	Bacteria Concentration (After BMPs)	Percentage Reduction
Catchments 1	273.43/ 330.93/ 332.38/ 431.77/ 370.08	182.65/ 221.05/ 222.02/ 288.41/ 247.21	33.2
Catchments 2	416.86 / 504.52/ 506.72 / 658.25/ 564.21	230.01/ 278.38/ 279.60/ 363.20/ 311.32	44.82
Catchments 4	374.06/ 452.71/ 454.70/ 590.66/ 506.28	187.86/ 227.36/ 228.36/ 296.64/ 254.26	49.77
Catchments 5	507.98/ 614.79/ 617.48/ 802.13/ 687.53	275.22/ 333.09/ 334.55/ 434.58/ 372.50	45.82
Catchments 6	296.09/ 358.35/ 359.92/ 467.54/ 400.75	149.64/ 181.11/ 181.90/ 236.30/ 202.54	49.45
Catchments 7	234.48/ 283.79/ 285.03/ 370.26/ 317.37	134.63/ 162.94/ 163.65/ 212.59/ 182.22	42.58
Catchments 11	533.55/ 645.73/ 648.56/ 842.49/ 722.13	271.04/ 328.02/ 329.46/ 427.98/ 366.84	49.2

It is crucial to understand the mechanisms associated with the consequences of climate change and flood severity and duration to address their impacts on the water quantity and quality attributes of catchments with various physical characteristics. Our study suggests that a primary source of non-point source pollution is likely to be the availability of on-site sewage facilities and their chance of failure due to their operational age and exposure to extreme climate events. The application of BMP structures is proposed to enhance the water quantity and quality measures. Furthermore, the presence of wet detention ponds is considered to diminish the adverse impact of flooding by lowering the peak runoff and bacteria concentration, respectively. The numerical framework developed in this thesis can be applied to other watersheds.

5. CONCLUSION

Wet detention pond in Neches River watershed has been implemented in SWMM model under 25-, 50-, and 100-years design storms to illustrate the changes in the peak stormwater flow reduction. Investigation of the cost-effectiveness of wet detention pond application to control water quantity and non-point source pollution during flooding is conducted by proposing three scenarios. The density of OSSFs in the catchments is considered the main factor in prioritizing the selection of catchments in these scenarios. A threshold value of approximately 40 percent is considered for peak flow reduction of generated runoff within the catchments to do the analysis. In each scenario, the application of detention pond between 1 – 5 % by catchment area reduces by roughly 40 percent in the peak flow. The application of each scenario will be greatly influenced by the given budget and the availability of land for implementing these wet detention ponds. It should be mentioned that the future study on evaluating the effect of detention pond implementation on the improvement of stormwater quality can also provide sufficient evidence on best scenario selection. In the second part of this analysis, the MOPUS model is integrated into the SWMM model to estimate the bacteria concentration within the catchments of the area of interest. Given three defined scenarios and corresponding catchments, the percentage reduction in bacteria concentration within seven catchments is obtained between 35-60 percent.

The followings are the summary of the most important findings acquired in this analysis:

- Different design storms have been generated and compared with the past extreme events to estimate the probable recurrence interval.
- Stormwater infrastructures have been integrated into the SWMM model through the implementation of wet detention ponds for mitigating the local runoff.

- Design storms of 25, 50, and 100 years have been selected to perform a cost-benefit analysis of the BMP implementation.
- Three scenarios for implementing the BMPs have been defined based on the number of the OSSFs within the catchments to give stakeholders alternatives for considering each.

This evaluation could be enhanced by filling the gaps and providing the following suggestions for future work:

- There was no flow data available, making it difficult to calibrate and validate the model to substantiate the outcome of simulation data with experimental observations. There is a need to install the streamflow gauge stations in the tributaries of the Neches River to obtain flow data and consider the model's well-defined initial conditions
- Not enough bacteria data was available to trace bacteria concentration for the MOPUS model. Therefore, there is a need to continuously monitor the water quality related to bacteria loading, specifically after extreme events.
- Not confirmed data was available to justify that OSSFs are the predominant cause for non-point source pollution.
- Integrate a module to SWMM to model vegetation type.
- Address the reason for increasing bacteria concentration in the time of dropping flow and no flooding scenarios.
- In application of MOPUS model integrated to SWMM model, try to integrate the number of OSSFs to estimate the bacteria concentration.

6. REFERENCES

Abu-Zreig, M., Rudra, R. P., Lalonde, M. N., Whiteley, H. R., & Kaushik, N. K. (2004). Experimental investigation of runoff reduction and sediment removal by vegetated filter strips. *Hydrological Processes*, *18*(11), 2029–2037.

Agriculture, U. S. D. of. (1986). Natural Resources Conservation Service. *Urban Hydrology for Small Watersheds*.

Bedan, E. S., & Clausen, J. C. (2009). Stormwater runoff quality and quantity from traditional and low impact development watersheds 1. *Jawra Journal of the American Water Resources Association*, *45*(4), 998–1008.

Berndtsson, J. C. (2010). Green roof performance towards management of runoff water quantity and quality: A review. *Ecological Engineering*, *36*(4), 351–360.

Birkland, T. A., Burby, R. J., Conrad, D., Cortner, H., & Michener, W. K. (2003). River ecology and flood hazard mitigation. *Natural Hazards Review*, *4*(1), 46–54.

Blake, E. S., & Zelinsky, D. A. (2018). National Hurricane center tropical cyclone report: Hurricane Harvey. *National Hurricane Center, National Oceanographic and Atmospheric Association*.

Chui, T. F. M., Liu, X., & Zhan, W. (2016). Assessing cost-effectiveness of specific LID practice designs in response to large storm events. *Journal of Hydrology*, *533*, 353–364.

Coombes, P. J., Argue, J. R., & Kuczera, G. (2000). Figtree Place: a case study in water sensitive urban development (WSUD). *Urban Water*, *1*(4), 335–343.

D'Arcy, B., & Frost, A. (2001). The role of best management practices in alleviating water quality problems associated with diffuse pollution. *Science of the Total Environment*, *265*(1–3), 359–367.

Dalton, P. A., Smith, R. J., & Truong, P. N. V. (1996). Hydraulic characteristics of Vetiver hedges: an engineering design approach to flood mitigation on a cropped flood plain. *Proceedings of the First International Vetiver Conference; Chiang Rai, Thailand*, 65–73.

Damodaram, C., & Zechman, E. M. (2013). Simulation-optimization approach to design low impact development for managing peak flow alterations in urbanizing watersheds. *Journal of Water Resources Planning and Management*, *139*(3), 290–298.

Davis, A. P. (2005). *Green engineering principles promote low-impact development*. ACS Publications.

Environmental Protection Agency. (2004). *Primer for Municipal Wastewater Treatment Systems*. US Environmental Protection Agency Municipal Support, Division Office of ….

Few, R. (2003). Flooding, vulnerability and coping strategies: local responses to a global threat. *Progress in Development Studies*, *3*(1), 43–58.

Gassman, P. W., Arnold, J. J., Srinivasan, R., & Reyes, M. (2010). The worldwide use of the SWAT Model: Technological drivers, networking impacts, and simulation trends. *21st Century Watershed Technology: Improving Water Quality and Environment Conference Proceedings, 21-24 February 2010, Universidad EARTH, Costa Rica*, 1.

Giacomoni, M. H., & Joseph, J. (2017). Multi-objective evolutionary optimization and Monte Carlo simulation for placement of low impact development in the catchment scale. *Journal of Water Resources Planning and Management*, *143*(9), 4017053.

Gros, M., Blum, K. M., Jernstedt, H., Renman, G., Rodríguez-Mozaz, S., Haglund, P., Andersson, P. L., Wiberg, K., & Ahrens, L. (2017). Screening and prioritization of micropollutants in wastewaters from on-site sewage treatment facilities. *Journal of Hazardous Materials*, *328*, 37–45.

Guto, S. N., Pypers, P., Vanlauwe, B., de Ridder, N., & Giller, K. E. (2011). Tillage and vegetative barrier effects on soil conservation and short-term economic benefits in the Central Kenya highlands. *Field Crops Research*, *122*(2), 85–94.

Hamel, P., Daly, E., & Fletcher, T. D. (2013). Source-control stormwater management for mitigating the impacts of urbanisation on baseflow: A review. *Journal of Hydrology*, *485*, 201–211.

Harrell, L. J., & Ranjithan, S. R. (2003). Detention pond design and land use planning for watershed management. *Journal of Water Resources Planning and Management*, *129*(2), 98–106.

Haydon, S., & Deletic, A. (2006). Development of a coupled pathogen-hydrologic catchment model. *Journal of Hydrology*, *328*(3–4), 467–480.

He, L.-M. L., & He, Z.-L. (2008). Water quality prediction of marine recreational beaches receiving watershed baseflow and stormwater runoff in southern California, USA. *Water Research*, *42*(10–11), 2563–2573.

Hegar, G. (2018). *A storm to remember*.

https://www.weather.gov/media/hgx/climate/summary/August_Climate_Article_2012.pdf. (n.d.).

Huntington, K. W., Blythe, A. E., & Hodges, K. V. (2006). Climate change and Late Pliocene acceleration of erosion in the Himalaya. *Earth and Planetary Science Letters*, *252*(1–2), 107–118.

James, R. J. E., & Ferguson, E. (2020). The dynamic relationship between pain, depression and cognitive function in a sample of newly diagnosed arthritic adults: a cross-lagged panel model. *Psychological Medicine*, *50*(10), 1663–1671.

Karamouz, M, Taheri, M., Mohammadi, K., Heydari, Z., & Farzaneh, H. (2018). A New

Perspective on BMPs' Application for Coastal Flood Preparedness. *World Environmental and Water Resources Congress 2018*, 171–180. https://doi.org/10.1061/9780784481431.018

Karamouz, Mohammad, & Farzaneh, H. (2020). Margin of Safety Based Flood Reliability Evaluation of Wastewater Treatment Plants: Part 2-Quantification of Reliability Attributes. *Water Resources Management*, *34*, 2043–2059.

Karamouz, Mohammad, Farzaneh, H., & Dolatshahi, M. (2020). Margin of Safety Based Flood Reliability Evaluation of Wastewater Treatment Plants: Part 1 – Basic Concepts and Statistical Settings. *Water Resources Management*, *34*(2), 579–594. https://doi.org/10.1007/s11269-019-02465-8

Kim, M. H., Sung, C. Y., Li, M.-H., & Chu, K.-H. (2012). Bioretention for stormwater quality improvement in Texas: Removal effectiveness of Escherichia coli. *Separation and Purification Technology*, *84*, 120–124.

Kossin, J. P. (2018). A global slowdown of tropical-cyclone translation speed. *Nature*, *558*(7708), 104–107.

Lavers, D. A., Ralph, F. M., Waliser, D. E., Gershunov, A., & Dettinger, M. D. (2015). Climate change intensification of horizontal water vapor transport in CMIP5. *Geophysical Research Letters*, *42*(13), 5617–5625.

Liu, R., Zhang, P., Wang, X., Chen, Y., & Shen, Z. (2013). Assessment of effects of best management practices on agricultural non-point source pollution in Xiangxi River watershed. *Agricultural Water Management*, *117*, 9–18.

McCarthy, D. T., Deletic, A., Mitchell, V. G., & Diaper, C. (2011). Development and testing of a model for Micro-Organism Prediction in Urban Stormwater (MOPUS). *Journal of Hydrology*, *409*(1–2), 236–247.

McCarthy, D. T., Mitchell, V. G., Deletic, A., & Diaper, C. (2007). Escherichia coli in urban stormwater: explaining their variability. *Water Science and Technology*, *56*(11), 27–34.

McIntyre, J. K., Davis, J. W., Hinman, C., Macneale, K. H., Anulacion, B. F., Scholz, N. L., & Stark, J. D. (2015). Soil bioretention protects juvenile salmon and their prey from the toxic impacts of urban stormwater runoff. *Chemosphere*, *132*, 213–219.

Morrison, D. (2014). *Quantifying E. coli Discharge from Failing Onsite Sewage Facilities in the Dickinson Bayou Watershed, Texas*.

Muthukrishnan, Swama, Richard, F., & Sullivan, D. (2006). Types of best management practices. *The Use of Best Management Practices (BMPs) in Urban Watersheds*, 21–77.

Muthukrishnan, Swarna, & Selvakumar, A. (2006). Evaluation of retention pond and constructed wetland BMPs for treating particulate-bound heavy metals in urban stormwater runoff. *World Environmental and Water Resource Congress 2006: Examining the Confluence of Environmental and Water Concerns*, 1–13.

Napier, F., Jefferies, C., Heal, K. V, Fogg, P., Arcy, B. J. D., & Clarke, R. (2009). Evidence of traffic-related pollutant control in soil-based Sustainable Urban Drainage Systems (SUDS). *Water Science and Technology*, *60*(1), 221–230.

Panagopoulos, Y., Makropoulos, C., & Mimikou, M. (2011). Reducing surface water pollution through the assessment of the cost-effectiveness of BMPs at different spatial scales. *Journal of Environmental Management*, *92*(10), 2823–2835.

Roesner, L. A., Bledsoe, B. P., & Brashear, R. W. (2001). Are best-management-practice criteria really environmentally friendly? *Journal of Water Resources Planning and Management*, *127*(3), 150–154.

Rossman, L. A. (2010). *Storm water management model user's manual, version 5.0*. National Risk

Management Research Laboratory, Office of Research and ….

Roy, A. H., Wenger, S. J., Fletcher, T. D., Walsh, C. J., Ladson, A. R., Shuster, W. D., Thurston, H. W., & Brown, R. R. (2008). Impediments and solutions to sustainable, watershed-scale urban stormwater management: lessons from Australia and the United States. *Environmental Management*, *42*(2), 344–359.

Scholz, M., & Grabowiecki, P. (2007). Review of permeable pavement systems. *Building and Environment*, *42*(11), 3830–3836.

Shaver, E., Horner, R. R., Skupien, J., May, C., & Ridley, G. (2007). *Fundamentals of urban runoff management: Technical and institutional issues*. North American Lake Management Society.

Shaw, D. (2003). *EPA's Report on the Environment (2003 Draft)*.

Srivastava, P., Hamlett, J. M., Robillard, P. D., & Day, R. L. (2002). Watershed optimization of best management practices using AnnAGNPS and a genetic algorithm. *Water Resources Research*, *38*(3), 1–3.

Strauss, P., Leone, A., Ripa, M. N., Turpin, N., Lescot, J., & Laplana, R. (2007). Using critical source areas for targeting cost-effective best management practices to mitigate phosphorus and sediment transfer at the watershed scale. *Soil Use and Management*, *23*, 144–153.

Te Chow, V. (2010). *Applied hydrology*. Tata McGraw-Hill Education.

Trenberth, K. (2011). Changes in precipitation with climate change. *Climate Research*, *47*(1–2), 123–138. https://www.int-res.com/abstracts/cr/v47/n1-2/p123-138/

Vijayaraghavan, B., Ely, D. R., Chiang, Y.-M., García-García, R., & García, R. E. (2012). An analytical method to determine tortuosity in rechargeable battery electrodes. *Journal of The Electrochemical Society*, *159*(5), A548.

Vineyard, D., Ingwersen, W. W., Hawkins, T. R., Xue, X., Demeke, B., & Shuster, W. (2015).

Comparing green and grey infrastructure using life cycle cost and environmental impact: A rain garden case study in Cincinnati, OH. *JAWRA Journal of the American Water Resources Association*, *51*(5), 1342–1360.

Vitro, K. A., BenDor, T. K., Jordanova, T. V, & Miles, B. (2017). A geospatial analysis of land use and stormwater management on fecal coliform contamination in North Carolina streams. *Science of The Total Environment*, *603*, 709–727.

Zhen, X.-Y. “Jenny,” Yu, S. L., & Lin, J.-Y. (2004). Optimal location and sizing of stormwater basins at watershed scale. *Journal of Water Resources Planning and Management*, *130*(4), 339–347.